HHS Public Access

Author manuscript

Br J Pharmacol. Author manuscript; available in PMC 2024 October 01.

Published in final edited form as:

Br J Pharmacol. 2023 October ; 180(19): 2550–2576. doi:10.1111/bph.16145.

BQ788 Reveals Glial ETB_R Modulation of Neuronal Cholinergic and Nitrergic Pathways to Inhibit Intestinal Motility: ETB_R Signaling is Linked to POI

E. Mazzotta[1], **I. Grants**[1], **E. Villalobos-Hernandez**[1], **S. Chaudhuri**[1], **J. L. McClain**[2], **L. Seguella**[3], **D. M. Kendig**[4], **B. A. Blakeney**[4], **K. S. Murthy**[4], **Reiner Schneider**[5], **Patrick Leven**[5], **Sven Wehner**[5], **A. Harzman**[6], **J. R. Grider**[4], **B. D. Gulbransen**[2], **F. L. Christofi**[1]

[1]The Ohio State University, Wexner Medical Center, Dept. of Anesthesiology, Columbus, OH, USA

[2]Michigan State University, Department of Physiology, East Lansing, MI, USA

[3]Sapienza University of Rome, Department of Physiology and Pharmacology “V. Erspamer”, Rome, Italy

[4]Virginia Commonwealth University, Richmond, Department of Physiology & Biophysics, VA, USA

[5]University of Bonn, Department of Surgery, Bonn, Germany

[6]The Ohio State University, Wexner Medical Center, Department of GI Surgery, Columbus, OH, USA

Abstract

Background and Purpose: ET-1 signaling modulates intestinal motility and inflammation, but the role of ET-1/ETB_R signaling is poorly understood. Enteric glia modulate normal motility and inflammation. We investigated whether glial ETB_R signaling is a mechanism regulating neural-motor pathways of intestinal motility and inflammation.

Experimental Approach: We studied ETB_R signaling using: ETB_R drugs (ET-1, SaTX, BQ788), activity-dependent stimulation of neurons (high K^+-depolarization, EFS), gliotoxins,

Correspondence: Fievos L. Christofi, PhD, AGAF, Professor and Vice Chair of Research, Department of Anesthesiology, The Wexner Medical Center, The Ohio State University, 216 Tzagournis Medical Research Facility, 420 West 12th Avenue, Columbus, OH, 43210, Fedias.christofi@osumc.edu.

Author Contribution Statement:

FLC: Contributed to conceptualization, design of study, investigation, funding acquisition, formal analysis, project management, supervision, visualization and writing of the manuscript. EVH: Contributed to investigation, study design, formal analysis, validation, visualization, and writing of the manuscript. IG: Involved in supervision, investigation, methodology, resources, validation and data curation. JRG: Participated in the conceptualization, formal analysis, funding acquisition, investigation, project administration and writing of manuscript. KSM and JRG: Contributed to formal analysis, writing of manuscript. BDG: Involved in conceptualization, methodology, project administration, review and editing of manuscript. LS: Contributed to investigation, manuscript editing. AH: Involved in conceptualization, funding acquisition, investigation, and manuscript editing. RS, PL and SW: Participated in the investigation and review of manuscript.

COI statement: The authors have no conflicts of interest to declare. This paper adheres to the BJP guidelines for *Design and Analysis* for transparent reporting and scientific rigor of preclinical research.

We have followed the recommendations set out in the BJP editorials where they are relevant.

Ethics Approval Statement: Studies were approved under IACUC animal protocols 2020A00000041. Human tissue studies were approved under human IRB protocol 2020H0273 for enteric glial ETB_R signaling in postoperative ileus.

Permission to Reproduce Materials from other Sources: N/A

Tg(Ednrb-EGFP) EP59Gsat/Mmucd mice, cell-specific mRNA in Sox10CreERT2; Rpl22-HAflx or ChATCre; Rpl22-HAflx mice, Sox10^{CreERT2}::GCaMP5g-tdT, Wnt1^{Cre2}::GCaMP5g-tdT mice, muscle tension recordings, fluid-induced peristalsis, ET-1 expression, qPCR, western blots, 3-D LSM-immunofluorescence co-labeling studies in LMMP-CM and a POI model of intestinal inflammation (P<0.01 is significant).

Key Results: In the *muscularis externa* ETB_R is expressed exclusively in glia. ET-1 is expressed in RiboTag(ChAT)-neurons, isolated ganglia and intra-ganglionic varicose-nerve fibers co-labeled with peripherin or SP. Pharmacological analysis of neural evoked glial responses indicates that ET-1 release provides activity-dependent glial ETB_R modulation of Ca^{2+}waves. BQ788 reveals amplification of glial and neuronal Ca^{2+}responses and excitatory cholinergic contractions. The BQ788 effect is sensitive to L-NAME. Gliotoxins disrupt SaTX–induced glial-Ca^{2+}waves and prevent BQ788 amplification of contractions. ETB_R is linked to inhibition of contractions and peristalsis. Inflammation causes glial ETB_R upregulation, SaTX-hypersensitivity and glial amplification of ETB_R signaling. *In vivo* BQ788 (i.p.,1mg/Kg) attenuates intestinal inflammation in POI.

Conclusion and Implications: Enteric glial ET-1/ETB_R signaling provides dual modulation of neural-motor circuits to inhibit motility - It inhibits excitatory cholinergic neural-motor pathways and stimulates inhibitory nitrergic motor pathways. Amplification of glial ETB_R is linked to *muscularis externa* inflammation and possibly pathogenic mechanisms of postoperative ileus.

Graphical Abstract

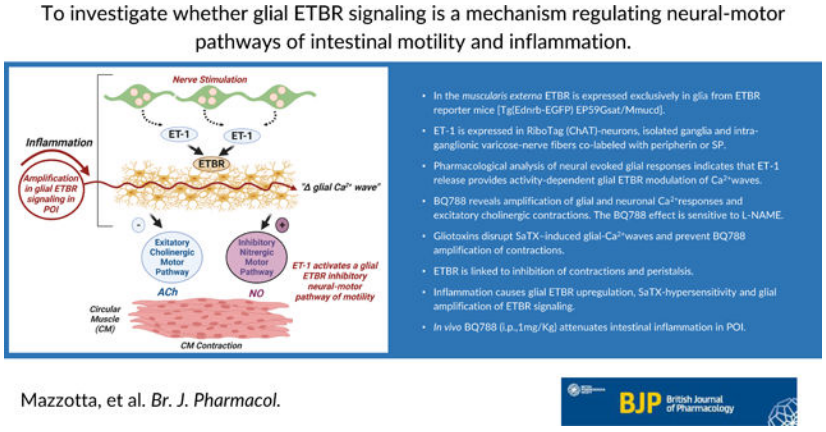

Introduction:

Endothelins exert their effects in health and disease by interacting with G-protein coupled ETA and ETB receptors (ETA_R and ETB_R). Endothelin signaling is implicated in numerous diseases including pulmonary hypertension, neurological diseases, inflammatory bowel disease (IBD), necrotizing enterocolitis, sepsis, acute pancreatitis and degenerative diseases.[1–7] Endothelin antagonists are approved for treatment of patients with advanced pulmonary hypertension.[1,8]

Endothelins are expressed in the gastrointestinal tract. Endothelin-1 (ET-1), ET-2 and ET-3 activate both receptors, although ET-1 is the predominant endothelin.[9–11] ETB_R signaling

is critical in the development of the enteric nervous system (ENS) and loss of ETB_R is linked to *aganglionosis* and Hirschsprung's Disease (HD).[12–14] Mutations of either ETB_R or ET-3 have been identified in animal models of HD[14] and in human[15–18]. However, little is known about ETB_R signaling in the adult gastrointestinal tract. Earlier studies suggested that activation of both ETA_R and ETB_R are involved in intestinal motility,[11,19,20] but the precise expression, distribution, and function of ETB_R signaling in the enteric nervous system (ENS) and intestinal motility is not known.

Studies in other peripheral ganglia and brain suggest that ETB_R signaling involves glia[6,21] and neurons[22,23]. Our preliminary study in ETB_R reporter mice (Tg(Ednrb-EGFP)EP59Gsat/Mmucd) showed that the EGFP reporter is expressed by enteric glia. Glia are important regulators of intestinal motility[24] and this motivated us to focus our attention on enteric glial ETB_R signaling and its role in motility. Glial activity encoded by intracellular Ca^{2+}responses is required for normal intestinal motility and function.[25–27] Disrupting glial Ca^{2+}responses inhibit motility and intestinal transit, while activating glial Ca^{2+}responses promote motility through interactions with neurons in gut motor circuits.[29–31]

'Reactive' enteric glial cells[32] are emerging as an important target of investigation in neurogastroenterology and motility for gastrointestinal diseases.[24,33–37] 'Reactive' glia are thought to be involved in pathogenic conditions associated with intestinal inflammation[38,39], enteric neuropathy[40], postoperative ileus[35], constipation[2], irritable bowel syndrome (IBS)[41,42], infection and diarrhea[24,38]. Glia are implicated in neurologic mechanisms of gut injury[43], as well as brain injury[44]. ET-1 and ETB_R in 'reactive' glia of the brain are implicated in pathogenic mechanisms of neurological diseases.[5,45]

We focused our investigation on whether glial ETB_R signaling is an important pathway in gut glial-neural motor pathways of motility and gut inflammation. The availability of more selective tools to study ETB_R signaling, including selective drugs such as BQ788 or sarafotoxin, Tg(Ednrb-EGFP)EP59Gsat/Mmucd mice, specific antisera against EGFP, ET-1 and ETB_R, cell-specific Ca^{2+}reporter mice for glia ($Sox10^{CreERT2}$;GCaMP5g-tdT) or neurons ($Wnt1^{Cre2}$;GCaMP5g-tdT) to monitor ENS activation, RiboTag mice, and spatiotemporal imaging of peristalsis, provided definitive ways to investigate ETB_R signaling in health or disease. To evaluate ETB_R signaling in 'reactive' glia, we used an established mouse model of postoperative ileus (POI) that is linked to *muscularis externa* (ME) inflammation and disruption of motility[35–37]. ETB_R signaling in human enteric glia was confirmed by Ca^{2+}imaging in glial networks obtained from surgical specimens. BQ788 reveals glial ETB_R modulation of neuronal cholinergic and nitrergic pathways to inhibit intestinal motility. ETB_R signaling is linked to POI and may represent a pathogenic mechanism.

2. Methods:

Animals:

All animal studies were approved by the IACUC Institutional Ethics committee on the use of animals at The Ohio State University, Michigan State University and Virginia

Commonwealth University. C57BL/6, six to eight weeks old male and female mice were purchased from Jackson Labs (Bar Harbor, ME). Mice were fed standard chow, water ad libitium. Mice for *in vitro* experiments were euthanized by CO_2 and cervical dislocation according to our approved protocols. C57BL/6J mice (Strain 000664) were used in organ bath experiments, *in vitro* fluid induced peristalsis, or *in vivo* studies with BQ788. Tg(Ednrb-EGFP)EP59Gsat/Mmucd reporter mice for ETB_R expression studies were obtained from Jackson MMRRC (STOCK Tg(Ednrb-EGFP)EP59Gsat/Mmucd, RRID:MMRRC_010620-UCD, was obtained from the Mutant Mouse Resource and Research Center (MMRRC) at University of California at Davis, an NIH-funded strain repository, and was donated to the MMRRC by Nathaniel Heintz, Ph.D., The Rockefeller University, GENSAT; cryopreserved and re-derived). The Tg(Ednrb-EGFP)EP59Gsat mouse contains the coding sequence for enhanced green fluorescent protein (EGFP), followed by a polyadenylation signal, inserted into the mouse genomic bacterial artificial chromosome (BAC) RP23–422M6 at the ATG transcription initiation codon of the endothelin receptor type B (Ednrb) gene so that expression of the reporter mRNA/protein is driven by the regulatory sequences of the mouse gene (J:100256).[46] Ca^{2+}reporter mice ($Sox10^{CreERT2}$;GCaMP5g-tdT and $Wnt1^{Cre2}$;GCaMP5g-tdT) were obtained from Dr. Brian Gulbransen and were bred at Michigan State University. They were shipped to our IACUC approved animal facility at OSU and kept in quarantine for 3 weeks to rule out any infection prior to use. Mice were maintained in a temperature-controlled environment on a 12-h light:dark cycle with access to water and mouse chow. Both male and female mice were used in the experiments.

Ca^{2+} reporter mice for glia and neurons:

Transgenic mice expressing the calcium indicator GCaMP5g selectively in enteric glia or in all enteric neurons and glia were generated by breeding *Sox10*^{CreERT2} mice[33] or *Wnt1*^{Cre2} mice (The Jackson Laboratory; https://www.jax.org/strain/022137; 129S4.Cg-*E2f1Tg(Wnt1-cre)2Sor*/J; RRID: IMSR_JAX:002137) with *PC::G5-tdTomato* mice (Jackson Labs 02447; B6;129S6-*Polr2aTn(pb-CAG-GCaMP5g,-tdTomato)Tvrd*/J; RRID: IMSR_JAX:024477[48]), respectively. The efficacy and specificity of the resulting *Sox10CreER*$^{T2+/-}$;*PC::G5-tdT*$^{+/-}$ (hereafter referred to as *Sox10*^{CreERT2}*;GCaMP5g-tdT*) and *Wnt1Cre2+/−;PC::G5-tdT+/−* (hereafter referred to as *Wnt1*^{Cre2}*;GCaMP5g-td*) have been described in prior work.[29,49] All double transgenic mice were maintained as heterozygous for both Cre and the GCaMP5g-tdTomato construct. CreERT2 activity was induced in *Sox10*^{CreERT2}*;GCaMP5g-tdT* mice by feeding the animals with chow containing tamoxifen citrate (400 mg/kg) for 1 week followed by 1 week of normal chow before use.[49] Mice of both sexes were used for experiments when they reached 8–12 weeks of age. Mice were maintained in a temperature-controlled environment on a 12-h light:dark cycle with access to acidified water and a minimal phytoestrogen diet (Diet Number 2919; Envigo, Indianapolis, IN) ad libitum. Genotyping was performed by Transnetyx (Cordova, TN).[49]

Chemicals:

Natural product research was not conducted in this study. All chemicals or drugs used were known compounds commercially available (>99% purity): Sarafotoxin S6c (cat #1175), BQ788 sodium salt (cat #1500), IRL 1620 (cat #1196), Tetrodotoxin (cat #1078),

Substance P (cat #1156), PPAD tetrasodium salt (cat #0625), and ARL67156 trisodium salt were purchased from Tocris Bioscience (Minneapolis, MN). Atropine sulfate salt monohydrate (cat #A0257), DL-Fluorocitric acid barium salt (cat #F9634), Adenosine 5' triphosphate disodium salt hydrate (cat #A26209), and Liberase (cat #05414451001) were purchased from Sigma Aldrich (St. Louis, MO). Carbamoylcholine chloride (carbachol, cat #ab141354) was purchased from Abcam (Waltham, MA). ET1 was purchased from American Peptide. DMEM/F12 (1:1) (cat # 11330–032; Fetal bovine serum (cat. # 26140–079), Penicillin-Streptomycin (5,000 U/mL) (Cat. #1507006); amphotericin B (cat # 15290–018), and Fluo-4 (cat # F14201) were purchased from Invitrogen, Thermo Fisher Scientific. Sodium Fluoracetate (cat # 201080) was purchased from MP Biomedicals.

Interventions and study design:

Tg(Ednrb-EGFP)EP59Gsat/Mmucd reporter mice and immunofluorescence co-labeling studies were used to study the distribution of the ET-1/ETB_R signaling pathway in the digestive tract. Real-time PCR and western blots confirmed gene transcripts and protein expression of ETB_R molecular forms in ME tissues (in normal or inflamed tissues). We tested the effects of ET-1 or the selective ETB_R agonist sarafotoxin S6c (SaTX) on enteric glia or neurons in Ca^{2+}reporter mice. High K^+ depolarization or EFS were used to study activity-dependent regulation of ET-1/ETB_R signaling in glia-to-neuron bi-directional communication. EFS contractions and fluid distension induced peristalsis were used to study the role of glial ETB_R in responses by disrupting glia with a gliotoxin (FC, 300μM; or FA, 5mM); the disruptive effect of gliotoxin on glial ETB_R was confirmed against SaTX-induced Ca^{2+}responses in glia. The physiological role of ETB_R was determined by testing the influence of the ETB_R antagonist BQ788 alone on intestinal tissues. BQ788 (1μM or 3μM) was incubated for 30 min to evaluate effects on glial Ca^{2+} responses, EFS responses, high K^+ depolarization induced responses, fluid induced peristalsis, muscle tension or phasic contractions. Gliotoxin was also incubated for either 30 min (FC), 90 min (or 4h) FA to disrupt glial functions and evaluate glial Ca^{2+} waves or muscle contraction.[47] L-NAME was incubated for 30 min to test if the inhibitory nitrergic signaling pathway is involved in the BQ788 effect. SaTX or ET-1 were incubated for 1–5 min to evaluate agonist effects at concentrations ranging from 0.5nM-100nM. In a postoperative ileus (POI) model of gut inflammation and abnormal motility, we tested whether ET-1/ ETB_R signaling was altered by evaluating ETB_R protein or mRNA expression, ETB_R expression in Ednrb-EGFP reporter mice, ET-1 dependent neuron-to-glial communication with high K^+ depolarization, or sensitivity to SaTX in glial Ca^{2+}waves. MPO or a panel of inflammatory markers were used to confirm inflammation in the POI model. *In vivo* administration of the ETB_R antagonist BQ788 was used to test whether ET-1 signaling contributes to intestinal inflammation in the mouse POI model.

Electrical Field Stimulation (EFS):

EFS was used to activate the ENS in the intact neural networks of enteric ganglia of cell-specific reporter mice for glia (*$Sox10^{CreERT2}$;GCaMP5g-tdT*) or neurons and glia *(Wnt^{Cre2};GCaMP5g-tdT).* An S48 Grass stimulator was used to deliver EFS trains of 0.1msec duration, 40V at 0.1Hz, 1Hz, 3Hz, 10Hz and 25 Hz frequencies, 3 min apart for a

5 sec duration. EFS was applied to tissues in a Quick-Release Low-Profile Field-Stimulation Chamber (RC-49MFSH, Warner Instruments, Hamden, CT).

High K^+ Depolarization:

A 75mM high K^+ solution balanced in osmolarity by subtracting Na^+ (*modified Krebs buffer solution substituting for NaCl*) was incubated with tissues for 2 min to trigger a Ca^{2+}response in glia.

Ca^{2+} Imaging:

Ca^{2+}imaging was done in cell-specific Ca^{2+}reporter mice or human enteric glia cells (hEGC). Methods for loading hEGC for Ca^{2+}imaging was described previously in our publications with minor in house modifications.[35,38,39] Briefly, hEGCs grown on a number zero coverslip in a 30 mm culture dish were incubated with 2 μM Fluo-4/AM (Invitrogen, Eugene, OR) in DMEM with no FBS for 30 min at 37°C and replaced with fresh media for an additional 30 min. At the end of this incubation, cells were placed on a stage of an up-right Nikon Eclipse FN1 microscope (Nikon, Tokyo, Japan) with a 20x-water immersion objective (Nikon Fluor, 0.50 n.a.) for Ca^{2+}imaging. A fluo-4 filter cube/dichroic set was used to capture fluorescence of fluo-4 loaded cells. The fluorescence Ca^{2+}signal was passed through an excitation filter model ET480/×40 center wavelength at 480-nm with 40-nm bandwidth, T510lpxrxt beamsplitter, and ET535/50-nm emission filter center at 535-nm with 50-nm bandwidth. For imaging in Ca^{2+}reporter mice, flat sheet preparations of LMMP ($0.8\times0.8cm^2$) were stretched over a piece of glass embedded in Sylgard and pinned flat, to allow visualization and imaging. The same imaging system was used for monitoring Ca^{2+} signals in Ca^{2+}reporter mice. Time-series images of Fluo-4 or GCaMP5g fluorescence (indicative of intracellular free $[Ca^{2+}]_i$ levels) were acquired at 7 frames/sec using an ANDOR iXon Ultra 897 EMCCD camera (Andor, Belfast, UK) controlled by NIS Elements Advanced Research software (Nikon, Tokyo, Japan). Cells were perfused with a peristaltic pump at 4 ml/min with oxygenated Krebs solution (mM: NaCl 120, KCl 6.0, $MgCl_2$ 1.2, NaH_2PO_4 1.35, $NaHCO_3$ 14.4, $CaCl_2$ 2.5, glucose 12.7) or SaTX (0.5nM – 20nM) diluted in Krebs buffer and applied by perfusion for 120 s. Recordings were made until the responses recovered to baseline. A “solution inline heater” (Warner Instruments, Inc., Hamden, CT) was used to maintain the perfusion temperature at 36.5°C ± 0.5°C. Glial cells were identified by tdTomato fluorescence in $Sox10^{CreERT2}$;GCaMP5g-tdT samples; tdTomato fluorescence was detected using excitation (535 nm, 20 nm) and emission (610 nm, 75 nm) band-pass filters. Neurons were identified and selected manually based on morphology, size, topography, and lack of tdT fluorescence and responsiveness to electrical stimulation (or high K^+ depolarization).

Isolation of glial cells from human specimens, purification and cultures of hEGC:

The IRB protocol was approved by the ethics committee of the College of Medicine at The Ohio State University to collect surgical tissue from colon of patients undergoing a colectomy (sigmoid colon removal for polyps or cancer); surgical tissue was collected from the non-pathologic margins. Informed consent was obtained before procurement of surgical tissue for the isolation and establishment of purified human enteric glial culture networks. Methods were described in detail in our previous publications.[38,50] Briefly, after cells

reach semi-confluence in 3 to 4 weeks, hEGC were enriched and purified by eliminating / separating fibroblasts, smooth muscle, and other cells. Glial cell enrichment and purification were achieved by labeling the isolated cells with magnetic microbeads linked to anti-D7-Fib specific antigen and passing them through a magnetic bead separation column following the manufacturer's instructions (Miltenyi Biotec Inc., San Diego, CA). This purification protocol was performed twice (P1 and P2) to reach a cell enrichment of up to 10,000-fold. Cells (> 95%) are strongly immunoreactive for the glial protein s100β and cells rarely label for α-smooth muscle actin (α-SMA).

Isolated networks of intact human myenteric ganglia:

Isolation of intact human networks of human myenteric plexus ganglia was done according to methods published by Grundmann et al.[51] Networks were loaded with 5μM fluo-4/AM for 45 min and rinsed with Krebs buffer for 45 min for Ca^{2+} imaging using the same Nikon Eclipse FN1 microscope imaging system described above.

Mouse Postoperative ileus model of *muscularis externa* inflammation:

The method for surgical gut manipulation is similar to that described previously[35,52] with a few in house modifications. Briefly, mice received a subcutaneous injection of 30 mg/kg Tramadol HCl 1h prior to surgery. The animal was placed on a heated pad (37^0C) and was anesthetized by inhalation of isoflurane (induced at 3%, 3 L/min flow and maintained at 2%, 2 L/min flow). A 1 cm midline incision was made to open the skin and peritoneum. The entire small bowel was gently removed/exteriorized from the peritoneal cavity, placed on sterile cotton gauze, and lightly manipulated by using two sterile moist cotton swabs two times from duodenum to terminal ileum. After intestinal manipulation (IM), the small bowel was carefully placed back in the cavity and the abdomen was closed by two layers of continuous sutures using 5.0 silk thread. The animal was awake and freely moving around the cage within 15 min. The operated mouse received a second dose injection of Tramadol HCl (30mg/kg) 2 h after the surgery and 1 mg/ml Tramadol HCl in drinking water was provided until they were sacrificed 3 h (3 h IM) or 24 h later (24 h IM). Control mice (no surgery), gut surgical manipulation (IM) or sham-operated animals (incision + anesthesia) were studied. Intestinal inflammation in the ME was identified by neutrophil infiltration (MPO^+ cells)[35] or inflammatory markers by Nanostring analysis[38].

In vivo intestinal transit with FITC-dextran:

Intestinal transit was evaluated *in vivo* by assessing the distribution of a 70 kDa FITC conjugated dextran marker (Sigma, St Louis, MO, USA) in the small intestine and colon of control, gut manipulate (IM), or sham-operated mice. Mice were fasted for 12 hours and then given 0.1 ml of 5mM FITC-dextran orally by gavage; after 90 minutes, mice were euthanized, and the small intestine was divided into 10 segments of equal length (S1–S10) and the colon into 4 equal segments labeled as C1–C4 from oral to distal colon and rectum. Each segment was flushed with 3 ml of 50 mM Tris buffered saline solution and samples were then centrifuged at 1200 rpm for 5min. The fluorescent activity of the supernatant was quantified using a fluorimeter at excitation 485nm and emission at 525nm. Intestinal transit was analyzed according to the intestinal mean geometric center (MGC) of the distribution of FITC-dextran throughout the intestines.[35,53]

Propulsive motility and spatiotemporal imaging:

Mouse colon segments were used to test the effect of distension with luminal fluids on peristaltic contractions. Colons were removed, mesentery trimmed, and placed in 20 ml perplex baths perfused with warmed, oxygenated Krebs buffer. Video cameras were placed over the segments which were transilluminated. After 30 min equilibration, peristalsis was initiated by intraluminal instillation of 5 μl Krebs buffer/mm of length. Video recordings were made for 1000 sec after which the intraluminal fluid was removed, and the preparation allowed to recover for 30 min with constant extraluminal perfusion with fresh Krebs buffer. After this period, the bath fluid was replaced with 20 ml Krebs containing 1 μM BQ788 or 50 nM SaTX or other drugs and video recordings were repeated. The data was analyzed, and spatiotemporal maps were made from all video recordings using the software associated with the GastroIntestinal Motility Monitoring system (GIMM; Catamount Research & Development, St Albans, VT). The width of the segment was represented in grey scale with a smaller diameter represented by lighter shades and wider diameter represented by darker shades. The number of peristaltic waves per 1000 s was calculated as waves moving in the oral-anal direction and the velocity of individual waves calculated in mm/s from the slope of each wave.[54]

Isometric Tension Recordings of circular muscle:

In vitro isometric muscle tension recordings in the circular muscle (CM) direction were recorded using a Radnoti tissue organ bath system (Radnoti LLC, Covina, CA) using 5 ml volume baths. Mouse colon LMMP-CM preparations were used with mucosa and submucosa carefully dissected away under a microscope. LMMP-CM tissue is cut into strips of ~3mm x 8mm in the circular muscle direction. The tissue is tied-off at both ends with a suture and hung in the circular muscle direction. It is then stretched to 0.5g of tension and allowed to equilibrate for 1h, draining and refilling the bath every 15 min. before starting studies. Electrical field stimulation was applied at frequencies ranging from 0.5 to 30Hz (60V, 0.5ms pulse duration). A 10 sec stimulation is applied using a Grass 48S stimulator (Grass Medical Instruments, Quincy, MA) at 5 min intervals. EFS elicits a CM contraction. The ETB_R antagonist BQ788 (3uM) is incubated alone for 30 min to test whether ET-1 exerts a physiological effect on CM contractions. Carbachol (100μM) or substance P (1μM) responses at the end of the experiment are used to normalize EFS responses. Atropine (10μM) or TTX (1μM) are applied for 15 min to determine the effects on EFS responses.

ET-1/ETB_R expression in the digestive tract:

For ETB_R expression, Tg(Ednrb-EGFP)EP59Gsat /Mmucd reporter mice were used to identify the cellular distribution and expression of ETB_R in the intestinal wall. EGFP expression is linked to ETB_R expression. Localization of ETB_R in different types of cells was identified by co-labeling studies for ET-1, HuC/D, S100β, GFAP, α-SMA, and chromogranin A. An antiserum for EGFP was used to confirm which cells express detectable levels of EGFP-immunoreactivity in Tg(Ednrb-EGFP)EP59Gsat/Mmucd reporter mice that may have low level EGFP expression.

Co-labeling studies for ET-1 and/or ETB_R were done in whole mount microdissected LMMP-CM intestinal tissues from wild-type mice, Tg(Ednrb-EGFP)EP59Gsat/

Mmucd reporter mice for ETB_R using EGFP fluorescence expression, or $Sox10^{CreERT2}$;GCaMP5gtdT mice with tdT^+ enteric glia. Isotopic antibodies for primary antisera or pre-absorption with control peptides for the immunogenic site of the antibody, if available, were used as controls; omission of primary antibodies was used as a control for secondary antibodies. Neither primary antibody nor secondary antibody dilutions were reused.

The following antibodies were used for immunofluorescent staining and Western blot studies (Supplement Table 1). The primary antibodies used were : Endothelin B receptor (Alomone, Cat # AER-002, RRID: AB_203984); Endothelin B receptor (Abcam, Cat # ab117529, RRID: AB_1090207); Endothelin B receptor (GeneTex, Cat # GTX17408, RRID: AB_374462); Rabbit Isotype control (Invitrogen, Cat # 31235, RRID: AB_243593); Chicken Isotype control (Abcam, Cat. # ab50579, RRID: not available); Anti-GFP (Abcam, Cat # ab13970, RRID: AB_300798); Smooth muscle actin, Clone EPR5368 (Abcam, Cat # ab124964, RRID: AB_11129103); Endothelin 1 (Abcam, Cat # ab113697, RRID not availabe); HuC/HuD, Clone EPR19098 (Abcam, Cat # ab184267, RRID: AB_2864321); S100 beta, Clone 4C4.9 (Abcam, Cat # ab4066, RRID: AB_304258); S100 beta, Clone EP1576Y (Abcam, Cat # ab52642, RRID: AB_882426); MHCII (Novus, Cat # NBP2–45312, RRID not available); MPO (Abcam, Cat # ab9535, dil: 1:100, RRID: AB_307322); CD68, Clone FA-11 (Bio-Rad, Cat # MCA1957T, RRID: AB_322219): Peripherin (Novus, Cat # NBP1–05423, RRID: AB_1556333); GFAP (Abcam, Cat # ab4674, RRID: AB_304558), and Chromogranin A (Abcam, Cat # ab15160, RRID: AB_301704). The following secondary antibodies were used immunofluorescent staining (diluted 1:400): donkey anti-rabbit, Alexa 488 (Invitrogen, Cat # A21206, RRID: AB_2535792); donkey anti-mouse, Alexa 488 (Invitrogen, Cat # A21202, RRID: AB_141607); donkey anti-mouse, Alexa 568 (Invitrogen, Cat # A10037, RRID: AB_2534013); donkey anti-rat, Alexa 488 (Invitrogen, Cat # A21208, RRID: AB_2535794); goat anti-chicken, Alexa 568 (Invitrogen, Cat # A11041, RRID: AB_2534098); goat anti-rabbit, Cy5 (Invitrogen, Cat # A10523, RRID: AB_2534032), and NucBlue Fixed Cell Ready Probe Reagent (DAPI) (ThermoFisher, Cat # R37606, 2drops/1 ml). The following secondary antibodies were used for Western blots (dilution 1:5000): donkey anti-mouse, IRDye 680RD (Li-Cor, Cat # 926–68072, RRID: AB_10953628); donkey anti-rabbit, IRDye 800CW (Li-Cor, Cat # 926–32212; RRID: AB_621847); donkey anti-goat, IRDye 680RD (Li-Cor, Cat # 926–68074, RRID: AB_10956736); donkey anti-chicken, IRDye 680RD (Li-Cor, Cat # 926–68075, RRID: AB_10974977). Note: The 3 different ETB_R antibodies tested were not suitable for immunofluorescent labeling in the mouse gut; however, they were suitable for western blots for ETB_R (see Fig. 1). Another antibody raised in sheep was used to label ETB_R in trigeminal ganglion neurons[23], but this antibody is no longer available from the company.

3-D imaging of co-labeled cells:

A Nikon A1R confocal imaging system was used for z-stack imaging and 3-D reconstructions of co-labeled cells in intact LMMP preparations of the mouse. Cells were imaged on the stage of a Ti2e fully motorized inverted microscope with a motorized XY stage visualized through a 60X oil immersion objective (1.20n.a.) with a working distance of 0.15–0.18 mm. The LU-NV series laser unit provided the excitation / emission spectra for

GFP (ex.487; em.500–550), Texas Red (ex. 561, em.570–620), Alexa 647 (ex.639, em.663–738), and DAPI (ex.402, em.425–475). A Galvano scanner was used to scan images, and z-stack images were acquired at 0.3μm steps; optical slice thickness ranged from 10–30μm depending on paraffin or tissue preparation, and layers being imaged. Image resolution was at 1024 × 1024 pixels, images were averaged 2x, and the pinhole was set at 0.8–1.2. Images were processed using NIS-Elements AR software.

Protocol for immunofluorescence co-labeling studies in tissues:

Microdissected LMMP-CM tissues were fixed in 4% PFA overnight and remaining CM was removed the next day. Tissues were washed with 1X PBS, 3 times, at 15 min intervals, on a horizontal shaker at room temperature, and then blocked with 0.5% Triton and 10% NDS at room temperature for 1 h. The blocking solution was discarded, and primary antibody was added (diluted in 1% NDS and 0.5% Triton). Tissue was incubated for 48 h at 4^{o}C. The excess primary antibody was washed off with 1X PBS, 3 times at 15 min intervals as noted before. Secondary antibody was added (diluted in 1% NDS and 0.5% Triton) and incubated at room temperature for 2 h in the dark. Tissues was washed as before and then incubated with DAPI for 10 min at room temperature in the dark followed by a 1 min wash in 1X PBS. The tissues were then mounted on slides and coverslips applied with Fluoromount (#0100–01, SouthernBiotech, Birmingham, AL).

Immunofluorescent co-labeling of Ednrb-EGFP mouse in paraffin sections:

To rehydrate and de-paraffinize tissue, sections were immersed in Citrisolv twice for 3 min each, then transferred to 100%, 95%, 70% ethanol consecutively for 3 min each. Sections were transferred to deionized water twice, for 3 min each. Once the rehydration steps were completed, the slides containing the sections were transferred to a Coplin jar containing sodium citrate buffer (pH 8.0) and heated to 97^{0}C in an oven for 30 min. After the incubation, the slides were cooled in the buffer for 20 min. For tissue permeabilization, Kimwipes and Q-tips were used to dry the area around the tissue sections on the slides. A square area was drawn around each of the sections with a hydrophobic PAP pen. The tissues were washed with 1X PBS, 3 times for 15 minutes each. Permeabilization buffer was added to the tissues (0.5% Triton in 1X PBS) and kept at room temperature for 30 min. Tissues were incubated at room temperature with the blocking buffer (10 % NDS, 0.5% Triton in 1X PBS) for 1 h. Primary antibodies were added to the antibody solution (1% NDS, 0.5% Triton, 1X PBS). Antibodies were incubated with tissue sections overnight at 4°C. The sections were washed 3x with 1X PBS for 15 min each. Secondary antibodies were incubated for 2 h in the dark and followed by washing the sections 3 time with 1X PBS, 15 min each in the dark. DAPI is added as a counterstain for nuclei.

Western Blot protocol

Samples were thawed on ice and then ground with mortar and pestle, keeping the mortar on ice. A volume of 200 μl of RIPA buffer (Catalog Number- 89901, Thermo Scientific, Rockford, IL) plus protease inhibitor (Catalog Number-78430, Thermo Scientific, Rockford, IL);100:1) was added to the ground sample and the whole homogenized mixture was transferred to an Eppendorf tube. The tube was kept on ice for 30 min and then centrifuged

at 13,000 rpm for 20 min at 4ºC. The supernatant was collected for further analysis or stored at −80ºC.

The OD for each sample was measured in a Perkin Elmer Victor 3 1420 Multilabel counter. Samples were mixed with 4X Laemli Buffer (4:1) and then boiled in a water bath for 10 minutes and kept on ice. Either 15µl or 50µl capacity wells (Catalog Number- 4561096, BIO-RAD) SDS gel was used; a 5µl volume of protein marker/ ladder (Catalog Number- 1610374, BIO-RAD) was loaded onto one lane. The gel was run at a constant voltage of 65V for 1.5 h or until the dye font reached the bottom of the gel, at room temperature, in 1X Tris/Glycine/ SDS running buffer (Catalog Number- 1610732, BIO-RAD). After the gel was run, the Western Blot protein transfer apparatus was assembled. The PVDF membrane (Immobilon-FL, Catalog number-IPFL00010, BIO-RAD) was placed in 100% methanol for 5 min and then transferred to the 1X Western Blot Tris/Glycine running buffer (Catalog Number- 1610734, BIO-RAD) for 5 min. The apparatus was sandwiched as follows: A sponge on the black (cathode) side, filter paper on top, SDS gel with the proteins, PVDF membrane, filter paper, sponge. All the above were pre-wetted with the 1X Western Blot Tris/Glycine transfer buffer prior to stacking. The stack was placed in the gel apparatus, with the red side of the cassette facing the anode and the black side facing the cathode and filled with the transfer buffer. The protein transfer was run at a constant voltage of 20V overnight. For antibody staining, the membrane was blocked for 1 h at room temperature and then incubated with primary antibody overnight at 4^0C; a 5% milk (Blotting-Grader Blocker, Catalog number-1706404, BIO_RAD) in TBST was used as blocking reagent and the primary antibody was diluted in blocking reagent. The next day, the membrane was washed with PBST, 3 times, 5 min each and then incubated with secondary antibody in blocking buffer at room temperature for 2 h in the dark. The membrane was washed with PBST, 3 times, 10 min each.

Post image analysis:

Images were acquired using the LI-COR Odyssey DLx imaging system. Densitometry was calculated using the blots compared to the GAPDH bands in the ImageJ (FIJI) software. Expression of ETB_R or other proteins are expressed as a percent of GAPDH expression in the same samples and plotted as a histogram.

Real-time PCR analysis:

Real-time PCR mRNA analysis for endothelin transcripts was done from ME samples. Suppl. Table 2 lists the Taqman assays for endothelin signaling and glial markers. To perform the Real-Time PCR analysis, 1.05 µg of total RNA was retro-transcripted using the High Capacity cDNA Reverse Transcription kit (Life Technologies). According to manufacturing protocol, 1 µl of cDNA was combined with 9 µl of a premade mix that included the TaqMan® Fast Advanced Master Mix and the TaqMan gene expression assay (predesigned by Applied Biosystems). The Comparative real-time PCR was performed in triplicate, including no-template controls and analyzed using Quant Studio 12K Flex system. The Ct Average of each triplicate was used to perform the relative quantification analysis. RNA input was normalized using Mouse GAPDH (Mm99999915_g1) as a reference gene and the relative expression was calculated using the comparative Ct method.

RNA isolation method:

Samples are transferred in 5 ml Polystyrene Round-Bottom tubes with 1 ml Trizol and tissues are disrupted using a homogenizer mixer. This step was performed on ice. The samples were forced to pass through a 26G needle using an insulin syringe to complete the homogenization. The homogenized product was then incubated 5 min at room temperature and 0.2 ml of chloroform was added. The samples were mixed vigorously for 15 sec, incubated 3 min at room temperature and centrifuged 15 min at 12,000 x g at 4°C in a refrigerated centrifuge. The clear upper phase was recovered in a fresh tube. An equal volume of 70% ethanol was added to each sample, mixed vigorously for 10 sec and applied to an RNA clean-up and concentration column (Norgen Biotek Corp, product # 23600). According to the protocol, columns were spun 1 min at 3,500 x g followed by 1 min at 14,000 x g. The columns were washed 3 times using 400 µl of Wash A solution (provided in the kit and previously diluted with 100% Ethanol as per manufacturer's specifications) and spun 2 min at 14,000 x g to dry the column resin; a 50 µl volume of Elution Solution A was applied to the columns and, after 5 min at room temperature, they were spun 1 min at 200 x g followed by 2 min at 5,800 x g and 30 sec at 14,000 x g to collect total RNA. For maximum recovery, the eluted RNAs were transferred back to the column and subjected to the same protocol again.

RiboTag-based mRNA immunoprecipitation:

Cell-specific mRNA from glia and neurons was obtained from Sox10CreERT2;Rpl22-HAflx or ChATCre; Rpl22-HAflx mice small bowel ME according to previously published protocols [Technote]. Briefly, the small bowel was removed, the ME mechanically removed from the mucosal layer and placed in RNAlater (Thermo Fisher Scientific, product # AM7021). ME lysis was performed with a Precellys homogenizer (Bertin Instruments) at three times for 45 s at 5000 rpm followed by a 10 min spin down at 10000 x g, at 4°C. Cleared lysate was incubated with anti-HA antibody (Biolegend, product # 901503) for 4 h at 4°C, 7 rpm, followed by conjugation with 200 µl A/G dynabeads (Thermo Fisher Scientific, product # 88802) and incubated overnight at 4°C, 7 rpm. Beads were rinsed three times, ribosomes with mRNA eluted from the beads and mRNA extracted with a Qiagen micro kit according to the manufacturer's manual.

Data analysis:

Raw Ca^{2+} imaging files were analyzed with NIS Elements Advanced Research software where regions of interest (ROIs) were drawn around enteric glial cells and neurons within a ganglion and the relative fluorescence intensity was measured. Analysis and generation of traces were performed using GraphPad Prism 8 (GraphPad Software, La Jolla, CA). Averaged traces represent the average change in fluorescence (ΔF/Fo) over time for all glial cells and neurons within a single ganglion. $\Delta F/F_0$ indicates the peak intensity of the Ca^{2+}response. Responsive glia/ganglion or neurons/ganglion indicate the number of cells involved in the Ca^{2+}wave in the intact neural network. For qPCR (or western blots), GAPDH was used to normalize data for gene transcripts (or proteins) and data are presented as 2^-ΔCt. For organ bath studies, data were normalized to % of carbachol (or substance P) response added at the end of the experiments. ST imaging maps for fluid induced peristalsis

were analyzed for frequency of peristaltic waves and velocity of peristaltic waves (see motility section). Image-J software was used to evaluate co-localization of neuronal markers by immunofluorescence.

Data Analysis and Statistics:

Data were analyzed using GraphPad Prism 8 (GraphPad, San Diego, CA) and are reported as mean ± SEM. A p value of <0.01 was considered statistically significant; 'n' values (i.e. 'n' refers to the number of animals, numbers of ganglia or numbers of cultures analyzed in separate experiments) and statistical tests used are reported in the figure legends and results. Unpaired or paired t-tests were used to analyze data between 2 groups depending on the experimental protocol. A one-way ANOVA followed by multiple comparisons using Tukey's test was used to make multiple comparisons. In multi-group studies with parametric variables, post hoc tests were conducted only if F in ANOVA achieved a significance level of 0.001. Concentration-response curves to ET-1 or SaTX were analyzed by one-way ANOVA. Two-way ANOVA was used to analyze differences between multiple interventions at different frequencies of stimulation, and Sidak's multiple comparison test (i.e. Figs 7, 8, 9); a 2-way ANOVA using a mixed effects model was used when appropriate. Sample sizes were determined from previous experimental data using a power of 0.8 and a significance level of 0.01. A P value of 0.01 is the threshold for statistical significance for determining whether groups differ. Statistical analysis was undertaken only for studies where each group size was at least n=5. The declared group size is the number of independent values, and that statistical analysis was done using these independent values. Outliers were included in data analysis and presentation. Where western blotting or immunohistochemistry has been conducted the experimental detail provided conforms with BJP Guidelines (Alexander et al,2018:175(3):407–411). The manuscript complies with BJP's recommendations and requirements on experimental design and analysis (Curtis et al, 2018: BJP 175:987–993).

Nomenclature of Targets and Ligands

Key protein targets and ligands in this article are hyperlinked to corresponding entries in https://www.guidetopharmacology.org and are permanently archived in the Concise Guide to Pharmacology 2021/22 (Alexander et al, 2021).

3. Results:

The expression, distribution and localization of ETB_R (Ednrb) was determined in WT, Tg (Ednrb-EGFP) EP59Gsat/Mmucd mice and / or RiboTag (Sox10-EGC) mice.

1. Distribution and localization of ETB_R:

qPCR and protein expression of ETB_R: Quantitative PCR (qPCR) analysis identified mRNA transcripts in ME for ETB_R, ETA_R, ET-1, ET-3, ENTPD2, GFAP, s100β, GDNF, nestin, PLP and Sox10 (Fig. 1a). Expression of ETB_R is much greater than ETA_R (or glial makers, *p<0.01). RiboTag (Sox10-EGCs)[55] mice confirmed that ETB_R ribosomal mRNA expression is much greater than ETA_R (Fig. 1b, **p<0.001).

Protein analysis: An anti-ETB_R antibody revealed bands at 52kDa and 42kDa. Both bands were expressed in colon and jejunum ME (Fig. 1c). The 52kDa band represents ETB_R. The 42kDa band was arbitrarily given the name ETB_R1 since it is recognized by the anti-ETB_R antibody. Note: mucosa and HEK-293 cells also express the 52kDa band (data not shown as focus is ETB_R signaling in ME). ETB_R is not expressed in CM (Fig. 1d). Quantitative data for ETB_R protein expression is shown in Fig. 1e-g. ETB_R1(42kDa band) is absent from CM but is expressed in ME (Fig. 1f).

2. Tg(Ednrb-EGFP)EP59Gsat/Mmucd mice:

ETB_R expression was analyzed by quantifying the EGFP fluorescence in LMMP-CM from Tg(Ednrb-EGFP)EP59Gsat/Mmucd mice (Fig. 2). $EGFP^+$ cells were 31.1±2.14 cells/ganglion versus 1.47±1.22 cells/field outside the ganglia (Fig. 2a). Co-labeled $EGFP^+$/$s100\beta^+$ co-labeled cells made up 85.19±5.38% cells/ganglion (Fig. 2b, n=5–7 mice). The EGFP reporter is restricted to $s100\beta^+$glia in myenteric ganglia of the colon (Fig. 2a, b), jejunum and ileum (Suppl. Fig. 1). EGFP reporter is absent from HuC/D^+ neurons (Fig. 2b). Images showing EGFP expression are shown in Fig. 2c-k. EGFP reporter is co-localized with GFAP (Fig. 2e) or s100β (Fig. 2f-h) but not HuC/D (Fig. 2i). Using an antibody to EGFP, we could confirm that in ME, EGFP-immunoreactivity in Tg(Ednrb-EGFP)EP59Gsat/Mmucd mice is expressed only in glia. In gut mucosa, a few epithelial cells express EGFP (Fig. 2j, k).

WBs with either an anti-EGFP (Fig. 3a) or an anti-Ednrb (ETB_R) antibody (Fig. 3b) recognize the same protein in lysates of jejunum *ME.* The protein has a M.W. of ~90kDa which is higher than that of the Ednrb (ETB_R) in WT mice with a M.W. of 52kDa (Fig. 1c). The EGFP antibody does not recognize any protein in WT mice (Fig. 3c). 3-D imaging using the anti-GFP (EGFP) antibody confirmed that EGFP is expressed in glia (Fig. 3d-f, h) not neurons (Fig. 3g, h) or smooth muscle (Figs 3j-l).

3. Ca^{2+}waves are triggered by ETB_R activation in *Sox10^{CreERT2}; GCaMP5g-tdT mice*:

ETB_R signaling in enteric glia was investigated on glial Ca^{2+}waves in *Sox10^{CreERT2}; GCaMP5g-tdT mice.* The selective ETB_R agonist SaTX triggers a Ca^{2+}wave in tdT^+ glia (Fig. 4a-f). An example of individual glial cell Ca^{2+}transients in the Ca^{2+}wave for a single myenteric ganglion is shown in Fig. 4e. The average response of individual Ca^{2+} transients is used for quantitative analysis of peak Ca^{2+}intensity (ΔF/Fo). The Ca^{2+} wave triggered by SaTX does not appear to be sensitive to 1μM TTX. The TTX resistant response to SaTX is consistent with a direct effect on glia. (Fig. 4g-k). The Ca^{2+}response occurs in ~35 glia/ganglion in the colon (n= 5 animals; 25 ganglia analyzed; Fig. 4k). The Ca^{2+}response spreads to 75–80% of glia in intestine (Fig. 4l).

SaTX triggers a concentration-dependent Ca^{2+}response in glia (Suppl. Fig. 3a,b; ANOVA,*p<0.01). Pre-incubation with the ETB_R antagonist BQ788 (1μM) for 30 min blocks the Ca^{2+}wave triggered by SaTX (Suppl. Fig.3c,d,e, *p<0.01); BQ788 has no effect on resting Ca^{2+}levels ($[Ca^{2+}i]$) (Suppl. Fig. 3c), and washout of BQ788 restores SaTX responses. The SaTX response occurs faster in a smaller 0.5ml perfusion chamber (Suppl.

Fig. 3f). SaTX triggers a Ca^{2+}wave in a culture network of human myenteric glia (Suppl. Fig. 3g-h) or networks of human myenteric ganglia (Suppl. Fig. 3i-j).

4. ET-1 release from the ENS activates ETB_R signaling in enteric glia:

ET-1 Ca^{2+}responses via ETB_R: Endothelin-1 (ET-1) triggers a concentration dependent Ca^2 response in glia from $Sox10^{CreERT2}$; GCaMP5g-tdT mice. (Fig. 5a-e; $p<0.01$, 1 way - ANOVA). The selective ETB_R antagonist BQ788 (1μM) blocks the Ca^{2+}wave triggered by 50nM ET-1. Pre-incubation of the LMMP-preparation with BQ788 for 30 min prevents the ET-1 Ca^{2+}response. The ET-1 effect recovers with washout of BQ788 (Fig. 5f, g).

High K^+ Depolarization of neurons: High K^+ depolarization (75mM) of neurons was used to stimulate ET-1 release. High K^+ depolarization triggers two different Ca^{2+}waves separated by time (Fig. 5h) The Ca^{2+}transients in each ganglion were averaged for analysis of data in different ganglia (Fig. 5h,k). The first Ca^{2+}wave is blocked by TTX whereas the second wave is not sensitive to TTX (Fig. 5h). Pooled data is shown in Fig. 5i-j. BQ788 significantly blocks the first Ca^{2+}wave response (Fig. 5k-m). In the second Ca^{2+} wave, BQ788 only reduces the number of glia responding/ganglion. Our working model of the high K^+ depolarization response is illustrated in Fig. 5n.

ET-1 neuronal expression in the mouse muscularis externa of the mouse small intestine: The source of ET-1 in the ME was investigated by ET-1 immunoreactivity, RiboTag(ChAT)-Neurons[55] and neural networks of human myenteric ganglia.

ET-1-immunoreactivity is abundant in intra-ganglionic varicose fibers in myenteric ganglia (Suppl. Fig. 2). ET-1^+ nerve fibers are in close contacts with tdT^+ glia in myenteric ganglia (Suppl. Fig. 2a, yellow staining over tdT^+ glia). ET-1 is not expressed in HuC/D^+ neurons (Suppl. Fig. 2b). ET-1 immunoreactivity is expressed in both SP^+ and $peripherin^+$ varicose nerve fibers (Suppl. Fig. 2c-f). 3-D imaging of ET-1-ir in a thicker z-stack to image through the entire thickness of LMMP-CM shows ET-1 is mainly expressed in intra-ganglionic varicose fibers (Suppl. Fig.2g-i). Edn1 (ET-1) mRNA expression was confirmed in RiboTag ChAT-Neurons[55] (Suppl. Fig. 2j; n=8 animals/group). ET-1 protein was detectable in isolated human neural networks of myenteric ganglia (Suppl. Fig. 2k, l; n=8)[56].

ETB_R signaling inhibits peristaltic waves, phasic activity, and CM contractions, and induces CM relaxations:

(i) ET-1 modulation of fluid induced peristalsis: SaTX inhibits fluid induced peristaltic waves in the distal colon of the mouse (Fig. 6). Fig. 6b shows that 50 nM SaTX can reversibly inhibit peristaltic waves induced by increasing pressure in the lumen with fluid. (c) SaTX (15 min) and BQ788 (15 min) have opposite effects on fluid induced peristalsis. Pooled data indicate that SaTX inhibits both the frequency of the peristaltic wave and the velocity of propagation of the peristaltic wave (Fig. 6d, e).

(ii) Gliotoxin disrupts SaTX-induced glial Ca^{2+}waves: We used a gliotoxin (90 min treatment, 0.1mM fluoroacetate) to disrupt glial function to show that it can inhibit SaTX-

induced glial Ca^{2+}waves (Fig. 6f,g; p<0.01). This is in keeping with the concept that SaTX inhibition of peristalsis (or EFS-CM contractions) involves glial ETB_R activation.

(iii) Gliotoxin effects on fluid induced peristaltic waves: The gliotoxin fluoroacetate (FA, 90 min) causes a concentration–dependent inhibition of the peristaltic waves, mimicking the effect of SaTX. Therefore, it was not possible to use FA to study interactions between FA and SaTX to further clarify if disrupting glial functions can alter SaTX-responses on peristaltic waves. In mouse colon, FA (0.1mM) decreases the frequency of peristaltic waves from 5.1±0.3 waves / 1000 s to 3.75±0.49 waves/1000 s (p=0.0463); 1.0 mM FA decreases it to 2.3±1.0 waves/1000 s (**p=0.001) and 5mM FA reduced it to 1.7±1.0 waves / 1000 s (**p=0.0002, n=5 (or more) animals.

(iv) BQ788 enhances CM contractions to EFS by interacting with glial ETB_R: The physiological action of the selective ETB_R antagonist BQ788 is to enhance neuromuscular responses of the circular muscle (CM). *In vitro* experiments on CM contractions to EFS showed that 100nM SaTX could cause a significant, but modest, inhibition of 20Hz EFS-induced off-contractions of the CM (Fig. 7a-b). As shown, the response to SaTX becomes desensitized. The response to EFS is abolished by blocking nerve conduction with TTX (1μM). In separate experiments, SaTX inhibited 1Hz and 3Hz EFS responses (p<0.01, Fig. 7b). In contrast, BQ788 causes enhancement of the EFS response at frequencies ranging from 0.1Hz to 30Hz (Fig. 7c-f).

(v) Gliotoxin prevents BQ788 enhancement of EFS responses: To test whether the effect of BQ788 involves enteric glia, we used gliotoxin to disrupt glial functions in the ENS. The response to BQ788 (Fig. 7g) is prevented by gliotoxin treatment (see Fig. 7g-i). Gliotoxin alone augments the control EFS response in CM (Fig. 7h) and after gliotoxin treatment, the effect of BQ788 is no longer evident (Fig. 7i).

(vi) SaTX – induced transient CM relaxations: As shown in Suppl. Fig. 4a-d, SaTX (100nM) could induce transient CM relaxations. The mean time to initial response is 32.5±1.8 sec (n=10). Peak relaxation occurs after 48.5±4.1 sec (n=5). The response to SaTX was blocked by BQ788 (1μM, n=5) or TTX (1μM, n=5) (Suppl. Fig. 4e,f). In contrast, ET-1 induced direct CM contractions (Suppl. Fig. 4g, h, l) which could not be blocked by TTX (Suppl. Fig. 4i, n=5) or BQ788 (Suppl. Fig. 4k, n=5). Data is consistent with activation of ETB_R by SaTX in glia of the ENS to cause CM relaxations.

(vii) Influence of BQ788 on resting tension and phasic contractions: In 22 LMMP-CM preparations from 12 mice, BQ788 (1μM) had no effect on resting tension (Suppl. Fig. 5a-b). However, BQ788 could enhance phasic contractile activity in CM (Suppl. Fig. 5c-e) in 20/22 tissues. In 20/22 tissues, BQ788 increased phasic activity from 36.5±9.2 contractions / 5min sampling period to 86.2 ±8.9 contractions / 5 min (paired t-test, p<0.01). In 20/22 tissues, it significantly increased the amplitude of contractions from 0.079±.003 g tension to 0.146±.003 (p<0.01).

BQ788 reveals an inhibitory glial–neural motor pathway modulating excitatory cholinergic transmission to CM:

(i) BQ788 causes amplification of the EFS-induced glial Ca^{2+}waves: EFS-induced Ca^{2+} waves were studied in $Sox10^{CreERT2}$;GCaMP5g-tdT glial Ca^{2+}reporter mice as shown in Fig. 8. BQ788 enhanced the EFS Ca^{2+}wave response in glia of the intact myenteric plexus (Fig. 8a-e, $p<0.01$, n=10 ganglia, and 138 cells analyzed). The response to EFS is abolished by TTX (1μM, $p<0.01$) confirming neuron-to-glial communication (Fig. 8f, n=10 ganglia).

Neuron-to-glial communication involves purinergic signaling.[55] We tested if purinergic signaling accounts for the entire EFS response ranging from 0.1Hz – 25Hz EFS. The P2 receptor antagonist PPADS (30μM) significantly reduces the EFS response (Fig. 8g; n=10 ganglia) but does not block it entirely. Preventing the inactivation of endogenous ATP by ARL67156 (100μM) augments EFS responses (Fig. 8h; n=10 ganglia, $p<0.01$). ATP (100μM) triggers a Ca^{2+} wave response (Fig. 8i).

(ii) The ETB_R antagonist BQ788 enhances ENS activation: The precise link between glial ETB_R activation and enteric neuronal firing (glia-to-neuron communication) is not known. To probe this question, EFS induced Ca^{2+}waves in neurons were studied in $Wnt1^{Cre2}$;GCaMP5g-tdT Ca^{2+}reporter mice with BQ788. The peak intensity of the Ca^{2+}response in neurons was enhanced by BQ788 ($p<0.01$, Fig. 9a), whereas the number of responsive neurons per ganglion in the Ca^{2+}wave remained the same (Fig. 9b; n=9 separate experiments, ns).

(iii) BQ788 amplification of excitatory cholinergic transmission and inhibitory nitrergic transmission to CM: At the CM level, the BQ788 (1μM) amplification of EFS-induced CM contractions is mitigated by the muscarinic antagonist atropine (10μM) used to block excitatory muscarinic cholinergic responses (Fig. 9c). In contrast, BQ788 had no direct influence on muscle contraction caused by carbachol (Fig. 9d, 100μM). EFS responses are abolished by TTX indicating that BQ788 is enhancing excitatory cholinergic neuromuscular transmission. L-NAME treatment reveals that a major component of the BQ788 effect on cholinergic CM contractions is due to modulation of NO-dependent signaling (Suppl. Fig. 6a,b).

6. *Muscularis externa* inflammation in *POI* causes amplification in ETB_R signaling:

(i) Postoperative ileus model: Endothelins are implicated in the pathogenesis of a variety of diseases linked to intestinal inflammation.[1,3–7,28] To begin to address the role of ET-1/ETB_R signaling in the context of inflammation, we tested the hypothesis that ET-1/ETB_R signaling in 'reactive' glia[2,35–38,40,49] is altered after gut inflammation in a well characterized POI mouse model of *muscularis externa* inflammation induced by gut surgical manipulation (IM) [35–37] (Suppl. Figs. 7 & 8). In the POI model, inflammation (Figs 7&8) and disruption of motility (slower GI transit) are hallmarks of the disease. GFAP immunoreactivity (marker of enteric gliosis) is upregulated and there is immune cell activation (Suppl. Fig. 8a-l). Up regulation in various pro-inflammatory mediators also occurs in ME of the mouse jejunum in POI after gut manipulation (IM versus sham, during

acute phase at 3h IM) (Suppl. Fig.8m-v, $p<0.01$). GI transit is decreased from 10.0±0.8 to 3.0±0.8 (MGC, fluorescence units) ($p<0.01$, n=5 animals/group).[35]

iii) Hypersensitivity to SaTX response in enteric glia: Ca^{2+}imaging in $Sox10^{CreERT2}$;GCaMP5g-tdT Ca^{2+}reporter mice demonstrated that in the context of inflammation, there is hypersensitivity to the selective ETB_R agonist SaTX in enteric glia (Fig. 10a-d, $p<0.01$). The peak intensity of the Ca^{2+}response (Fig. 10c) and the number of glia/ganglion responding to SaTX in the Ca^{2+}wave (Fig. 10d) were both augmented in POI.

(iv) Upregulation of ETB_R: In POI, there is upregulation of the EGFP reporter visualized in glia of the Tg(Ednrb-EGFP)EP59Gsat/Mmucd mice in duodenum (Fig. 10e) and ileum (Fig. 10f) of the small intestine. This was confirmed by western blots for ETB_R protein for 3h and 24h IM (Fig. 10g-i). ETB_R1 is absent in IM animals in contrast to sham-controls (Fig. 10g-i). Pooled data for the expression of ETB_R (52kDa) and ETB_R1 (42kDa) show upregulation of ETB_R and absence of ETB_R1 after IM (Fig. 10i, $p<0.01$, n=5 animals/group). Data indicate that ET-1/ETB_R signaling is upregulated in POI.

(v) Amplification in ETB_R signaling is revealed with high K^+ depolarization in the POI model: To test whether ET-1/ETB_R signaling is altered in POI, we determined the effects of BQ788 on high K^+ depolarization induced Ca^{2+}waves in $Sox10^{CreERT2}$;GCaMP5g-tdT Ca^{2+}mice in POI (Fig. 10j-o). There is amplification of the first and second Ca^{2+}waves triggered by High K^+ (i.e. increase in $\Delta F/Fo$) in POI (Fig. 10j-o). For the first wave, BQ788 reduces the responses in sham and IM animals (Fig. 10k, l). BQ788 reduces the second wave response to high K^+ in IM, but not sham animals (Fig. 10 n, o). Overall, there is amplification in the high K^+ depolarization induced Ca^{2+} responses and these are sensitive to BQ788, implying that ET-1 signaling is augmented in POI. The proposed mechanism of amplification of ETB_R signaling by inflammation is illustrated in Fig. 10 q.

(vi) Upregulation of ETB_R in POI is restricted to glia in muscularis externa.: The EGFP reporter is upregulated in Tg(Ednrb-EGFP)EP59Gsat/Mmucd mice in POI (Suppl. Fig.9a-d). There is also upregulation of the protein recognized by both anti-EGFP (Suppl. Fig 9e-g) and anti-Ednrb (ETB_R) antibody (Suppl. Fig. 9h-j). 3-D imaging through the entire thickness of an LMMP-CM preparation confirmed that in the inflamed state the EGFP reporter is expressed (upregulated) in glia (Suppl. Fig. 9k-n). There is no co-localization of EGFP reporter with HuC/D-immunoreactivity in neurons (Image J, Suppl. Fig. 9o-p). EGFP reporter is highly co-localized with GFAP-immunoreactivity (Suppl. Fig. 9q-r). Overall, glial Ednrb (ETB_R) expression is upregulated in POI.

7. In vivo BQ788 administration inhibits inflammation in mouse POI—*In vivo*

i.p. administration of 1mg/Kg BQ788 daily for 7 days significantly inhibited leukocyte infiltration in the ME of the jejunum in the mouse POI model (Suppl. Fig. 7d-f; n=5 mice each; $p<0.01$ between IM and IM + BQ788).

4.0 Discussion:

Endothelins interact with G-protein coupled ETA_R and ETB_R to exert a variety of effects in normal and disease states, and are implicated in IBD, necrotizing enterocolitis, IBD, acute pancreatitis, neurological diseases and sepsis.[1,3–5,7,27,57] ETB_R signaling is critical in the development of the ENS and loss of ETB_R is linked to *aganglionosis* and HD.[12,13] Little was known about ETB_R signaling and its role in intestinal motility in adult mammals in normal or inflamed gut. The current study targeted the ETB_R in the ENS or 'little brain in the gut', that is essential for life and intestinal motility. Novel findings support the concept that glial ETB_R signaling is an important pathway in gut glial-neural motor pathways of motility and gut inflammation.

Earlier pharmacological studies on endothelin in guinea pig or rat suggested that ET-1 was involved in modulating motility, although the cellular distribution and function of ETB_R in neurons, glia or muscle were unclear.[9,11,19,20,58,59]. *Tg-Ednrb-EGFP reporter mice* [46] for Ednrb (ETB_R) were instrumental in the identification of ETB_R in the gut since antisera were not suitable for labeling ETB_R in gut tissues. EGFP is a quantitative reporter of gene expression or activity[46] in cells.[60–62] Enhanced Green fluorescent protein (EGFP) is visible with FITC in cells expressing ETB_R. Expression of Ednrb (ETB_R) in Tg(Ednrb-EGFP)EP59Gsat/Mmucd][46] was shown in astrocytes and it matches in situ data from the GENSAT Project[46]. For ME, EGFP reporter imaging (or EGFP-immunoreactivity) in Tg-mice confirmed that EGFP is only expressed in glia. Our data from RiboTag-Sox10-EGC mice[55]confirmed that ETB_R is the predominant endothelin-receptor in enteric glia. In Tg-mice, an anti-EGFP or an anti-Ednrb (ETB_R) antibody recognizes the same larger (~90kDa) protein compared to the ETB_R protein at 52kDa in WT-mice, implying that the larger protein is associated with both Ednrb and EGFP.

This discovery facilitated study of glial ET-1/ETB_R signaling in the regulation of motility. ETB_R is highly expressed in glia relative to the glial markers GFAP, s100β and PLP, and may represent a novel biomarker for enteric glia in adult mouse ENS. In other peripheral ganglia, there is variable expression of ETB_R in glia[6,21,63] and neurons[20]. Potential species or regional differences in ETB_R expression and function in the gut[11,19,20,59] deserve further investigation. Activation of ETB_R has also been shown to trigger Ca^{2+}waves in human enteric glia.[35,38,49]

ET-1 is the predominant endothelin activating ETB_R. In our study, ET-1 was shown to be specifically expressed in the mouse ENS, although it remains unknown whether ET-1 is expressed in both intrinsic and extrinsic nerve fibers.[3,64] There is co-labeling for ET-1 and SP^+ or peripherin$^+$ varicose nerve fibers in myenteric ganglia, neurons in RiboTag(ChAT)-neurons and isolated human networks of purified myenteric ganglia. This establishes the ENS as the primary source of endogenous ET-1 for glial ETB_R activation. The direct physiologic release of ET-1 remains to be proven. ET1-immunoreactivity was reported for human colon ENS.[10]

ET-1 immunoreactive nerve fibers are in close proximity to enteric glia, suggesting that if ET-1 is released, it could activate glial ETB_R. To test this hypothesis, we utilized high K^+

depolarization of neurons to induce glial activation. Neuron-to-glial transmission, triggered by high K^+ depolarization is blocked by the selective ETB_R antagonist BQ788, indicating that endogenous ET-1 release activates glial ETB_R to trigger a Ca^{2+}wave. Exogenous ET-1 or the selective ETB_R agonist SaTX triggers a robust Ca^{2+}wave by direct activation of glial ETB_R since the effect is blocked by BQ788, but not TTX. Potassium depolarization studies in glial-specific Ca^{2+}reporter mice suggest that neuronal release of ET-1 activates *glial ET-1/ETB_R signaling* to trigger glial Ca^{2+}waves.

Findings support the concept that neural ET-1 triggers activity-dependent regulation of glial Ca^{2+}waves since high K^+ depolarization or electrical stimulation elicit different and opposing effects on ETB_R signaling on glial Ca^{2+}waves. In contrast to high K^+ depolarization, the glial Ca^{2+}response evoked by electrical stimulation is amplified by BQ788, suggesting that endogenous ET-1 provides inhibitory modulation of the response.

Mechanistically, high K^+ depolarization and EFS act differently. High K^+ depolarization provides a slow sustained depolarization of neurons to increase intracellular Ca^{2+}levels leading to transmitter release to activate glia. Electrical stimulation exerts a phasic pattern of activation that is intermittent and frequency dependent, oscillating between activation and no activity. Potassium depolarization produces a non-physiologic membrane depolarization and tonic elevation of intracellular calcium, a condition that does not mimic cellular responses to physiologic patterns of phasic neuronal activity. Electrical stimulation is used to produce physiologic patterns of phasic neuronal activity.[65]Activity-dependent regulation of ionic conductance(s), gene expression and other neuronal functions occurs in response to these different patterns of stimulation.[66–67] These two modes of stimulation may reveal activity dependent regulation of glial ET-1/ETB_R signaling in mouse ENS. Information in the nervous system is coded in the temporal pattern of neural impulse firing. Depolarizing neurons with potassium chloride fails to produce the natural mode of information processing in neurons.[66–67] Activity-dependent regulation may also operate in disease states as discussed later for POI.

Our working hypothesis of the physiologic role of glial ETB_R signaling on intestinal motility is illustrated in Fig. 9e. BQ788 revealed an increase in phasic activity in CM, augmentation of CM contractions, and enhanced peristalsis. These effects suggest inhibitory modulation by endogenous ET-1 at ETB_R. Exogenous effects of SaTX (or ET-1) further corroborated our findings showing that ET-1/ETB_R activation causes transient relaxation of CM, inhibitory modulation of CM off-contractions to electrical nerve stimulation, and inhibition of peristalsis. Transient relaxation is likely to start with SaTX activation of ETB_R in glia. Our experiments were designed to test actions through ETB_R. Gliotoxins could prevent the effects of BQ788 on neuromuscular contractions and disrupt SaTX responses in glia. The glial ET-1/ETB_R pathway is involved in inhibitory modulation of excitatory cholinergic (and perhaps non-cholinergic[22,72]) neural motor circuits of intestinal motility.

At the ENS level, BQ788 alone caused amplification in glial and neuronal activation in response to EFS, although the precise mechanisms or pathways remain unknown.[73] Studies using Wnt-1 Ca^{2+}reporter mice indicate that BQ788 facilitates neural activity induced by electrical stimulation. BQ788 caused a robust increase in the peak intensity of the Ca^{2+}wave

response in neurons but had little effect on number of neurons/ganglion responding in the ganglia of the intact neural circuits of the ENS. Data is consistent with the concept of inhibitory modulation of an excitatory cholinergic neural motor circuit of motility. Circuit-specific enteric glia regulates intestinal motor neurocircuits.[29] Glial ET-1/ETB_R signaling could be linked to circuit specific excitatory motor pathways. Overall, the effect of BQ788 suggests that ETB_R are normally active and provide some inhibitory tone. In brain, astrocyte ETB_R activation was shown to either increase or decrease supraoptic nucleus firing activity via excitatory or inhibitory neurotransmitter pathways.[74]

Modulation of inhibitory nitrergic signaling pathways is another mechanism operating in the BQ788 amplification effect of cholinergic CM contractions:

L-NAME disruption of inhibitory nitrergic signaling reveals that a major component of the BQ788 effect on cholinergic CM contractions is due to modulation of NO-dependent signaling. There is also an L-NAME-insensitive component of the BQ788 effect (see Suppl. Fig. 6). Our working model of glial ET-1/ET_BR signaling in glia, ENS and motility is illustrated in Fig. 9e. Enteric glial ET-1/ETB_R signaling provides dual modulation of neural-motor circuits to inhibit motility. Endogenous ET-1 release from varicose nerve fibers activates glial ETB_R to inhibit Ca^{2+}waves[56]. Overall, ET-1 provides dual modulation of two distinct neural-motor circuits, resulting in glial inhibitory modulation of excitatory glial neural-motor pathways (*cholinergic pathway*) or activation of an inhibitory glial neural-motor pathway (*nitrergic pathway*).

To evaluate ETB_R signaling in 'reactive' glia[32, 24,34–38], we used a mouse model of POI linked to ME inflammation and disruption of motility[35–37,55]. We found there is *hypersensitivity* to glial ETB_R signaling and glial Ca^{2+}waves. Up regulation of ETB_R in glia likely contributes to the hypersensitivity and persists during 24h IM that is associated with dysmotility and POI. We provide evidence from the POI model that the larger protein that is recognized by both anti-EGFP and anti-Ednrb antibodies is highly upregulated in Tg(Ednrb-EGFP)EP59gsat/Mmucd mice. There is also amplification of the ET-1/ETB_R signaling in POI. *In vivo* pharmacological blockade of ETB_R with BQ788 reduces inflammation in POI, indicating that the ET-1/ETB_R signaling pathway is a potential pathogenic mechanism of dysmotility and POI. Enteric glia serve an essential role in intestinal function[25,26,75], motility and diseases.[24,25,28,34–38,42,75,76] Disruption of glial functions leads to abnormal intestinal motility.[58,76] Alterations in glial ET-1/ ETB_R signaling is a property of 'reactive' glia in the inflamed gut of POI as demonstrated in our study.

It remains unclear what the two different molecular forms of the protein are that are recognized by the anti- ETB_R antibody. It recognizes bands at 52kDa and at 42kDa. Different size proteins are expressed in different species[68,69] and different cells[70,71]. In mouse POI, it is interesting that only a single protein for ETB_R is expressed in ME at 52kDa. The 52kDa protein is upregulated in POI, and it is tempting to speculate that inflammation in the disease state, may prevent the ETB_R protein from further modifications to produce the truncated version of the ETB_R1 (42kDa protein) recognized by the antibody[66,67]. In diseases, perhaps post-translational modification[66,67] is inhibited

and a single ETB_R protein at 52KDa is expressed, but the molecular mechanisms remain speculative.

Summary and Conclusions:

In ME, ETB_R is expressed only in glia *and is sensitive to gut inflammation. It may represent a marker for glia and 'reactive' myenteric glia associated with upregulation of ETB_R in the adult mouse POI model.* Activity-dependent regulation of glial ETB_R signaling may occur in the mouse intestine. BQ788 revealed a novel pathway of glial ET1/ETB_R inhibitory modulation of excitatory cholinergic neural–motor pathways and activation of inhibitory nitrergic neural-motor pathways to inhibit intestinal motility. There is amplification of glial ETB_R signaling in POI. *In vivo* BQ788 attenuates intestinal inflammation. Enteric glial ETB_R signaling is a potential novel pharmacological target for intestinal motility disorders that can be probed further using inducible GFAP-CreER-ETB_R-cKO mice[44], rat mutants[77] or Piebald lethal mutant mice of ETB_R that survive to adulthood[78].

Supplementary Material

Refer to Web version on PubMed Central for supplementary material.

Acknowledgements:

We would like to acknowledge the efforts of two student trainees: Nick Paeglis was an undergraduate student volunteer at The Ohio State University in the Neuroscience Program. Kyle Hopkins was a summer medical student volunteer from Ohio Wesleyan University. They trained in immunofluorescent co-labeling techniques using the Tg(Ednrb-EGFP)EP59Gsat/Mmucd mice. We are grateful to the department of Anesthesiology for providing additional resources, MOU support for Biostatistics and a supporting environment to facilitate the NIH funded studies. Thank you to Dr. Kent Williams for providing some ETB_R reporter mice. Our appreciation goes out to the entire clinical research team in Anesthesiology for supporting our human patient IRB(s) studies.

This Declaration acknowledges that this paper adheres to the principles for transparent reporting and scientific rigour of preclinical research as stated in the *BJP* guidelines for Design and Analysis, Immunoblotting and Immunochemistry, and Animal Experimentation, and as recommended by funding agencies, publishers and other organisations engaged with supporting research.

Funding Statement:

FLC is the recipient of grants R01DK113943 and R01DK125809 from the National Institutes of Diabetes, Digestive and Kidney Diseases (NIDDK) on glial ETB_R signaling and glial modulation of postoperative ileus. BDG is the recipient of R01DK120862 and R01DK103723. JRG is the recipient of grants R01DK34153 and R01DK113943. KS Murthy is the recipient of grants R01DK15564 and R01DK28300.

Data Availability Statement:

The data included in this study will be made available from the corresponding author upon reasonable request. Some data from human subjects may be protected under the privacy/ HIPPA regulations.

Abbreviations:

CM	circular muscle
ATP	adenosine-5'-triphospate

SaTX	Sarafotoxin S6c
ET-1	endothelin-1
ET-2	endothelin-2
ET-3	endothelin-3
SP	substance P
ACh	Acetylcholine
CgA	chromogranin A
CM	circular muscle
EFS	electrical field stimulation
ENS	enteric nervous system
PCR	polymerase chain reaction
WB	western blot
ETA_R	Endothelin-A receptor
ETB_R	Endothelin-B receptor
KO	knock-out
ME	muscularis externa
FA	sodium fluoroacetate
FC	fluorocitrate
hEGC	human enteric glial cells
FBS	fetal bovine serum
IM	intestinal manipulation
MGC	mean geometric center
MPO	myeloperoxidase
NO	nitric oxide
POI	post-operative ileus
LMMP-CM	longitudinal muscle-myenteric plexus-circular muscle
TTX	tetrodotoxin

6. References

1. Angeli F, Verdecchia P, Reboldi G. (2021). Aprocitentan, A Dual Endothelin Receptor Antagonist Under Development for the Treatment of Resistant Hypertension. Cardiol Ther, 10(2):397–406. doi: 10.1007/s40119-021-00233-7. [PubMed: 34251649]
2. Bhave S, Gade A, Kang M, Hauser KF, Dewey WL, Akbarali HI (2017). Connexin-purinergic signaling in enteric glia mediates the prolonged effect of morphine on constipation. FASEB J, 31(6):2649–2660. doi: 10.1096/fj.201601068R. [PubMed: 28280004]
3. D'Orléans-Juste P, Akide Ndunge OB, Desbiens L, Tanowitz HB, Desruisseaux MS (2019). Endothelins in inflammatory neurological diseases. Pharmacol Ther, 194:145–160. doi: 10.1016/j.pharmthera.2018.10.001. [PubMed: 30291906]
4. Groesdonk HV, Raffel M, Speer T, Bomberg H, Schmied W, Klingele M, Schäfers HJ (2015). Elevated endothelin-1 level is a risk factor for nonocclusive mesenteric ischemia. J Thorac Cardiovasc Surg,149(5):1436–1442.e2. doi: 10.1016/j.jtcvs.2014.12.019. [PubMed: 25623906]
5. Hostenbach S, D'haeseleer M, Kooijman R, De Keyser J. (2016). The pathophysiological role of astrocytic endothelin-1. Prog Neurobiol, 144:88–102. doi: 10.1016/j.pneurobio.2016.04.009. [PubMed: 27132521]
6. Pomonis JD, Rogers SD, Peters CM, Ghilardi JR, Mantyh PW (2001). Expression and localization of endothelin receptors: implications for the involvement of peripheral glia in nociception. J Neurosci, 21(3):999–1006. doi: 10.1523/JNEUROSCI.21-03-00999.2001. [PubMed: 11157085]
7. Unlüer EE, Alican I, Yeğen C, Yeğen BC (2000). The delays in intestinal motility and neutrophil infiltration following burn injury in rats involve endogenous endothelins. Burns, 26(4):335–340. doi: 10.1016/s0305-4179(99)00135-7. [PubMed: 10751700]
8. Wei A, Gu Z, Li J, Liu X, Wu X, Han Y, Pu J. (2016). Clinical Adverse Effects of Endothelin Receptor Antagonists: Insights from the Meta-Analysis of 4894 Patients From 24 Randomized Double-Blind Placebo-Controlled Clinical Trials. J Am Heart Assoc, 5(11):e003896. doi: 10.1161/JAHA.116.003896.
9. Egidy G, Juillerat-Jeanneret L, Korth P, Bosman FT, Pinet F. (2000). The endothelin system in normal human colon. Am J Physiol Gastrointest Liver Physiol, 279(1):G211–222. doi: 10.1152/ajpgi.2000.279.1.G211. [PubMed: 10898765]
10. Inagaki H, Bishop AE, Escrig C, Wharton J, Allen-Mersh TG, Polak JM (1991). Localization of endothelin-like immunoreactivity and endothelin binding sites in human colon. Gastroenterology, 101(1):47–54. doi: 10.1016/0016-5085(91)90458-w. [PubMed: 2044926]
11. Shahbazian A, Holzer P. (2000). Regulation of guinea pig intestinal peristalsis by endogenous endothelin acting at ET(B) receptors. Gastroenterology, 119(1):80–88. doi: 10.1053/gast.2000.8549. [PubMed: 10889157]
12. Gariepy CE, Williams SC, Richardson JA, Hammer RE,Yanagisawa MY (1998). Transgenic expression of the endothelin-B receptor prevents congenital intestinal aganglionosis in a rat model of Hirschsprung disease. J Clin Invest,102(6):1092–1101. doi: 10.1172/JCI3702. [PubMed: 9739043]
13. Hosoda K, Hammer RE, Richardson JA, Baynash AG, Cheung JC, Giaid A, Yanagisawa M. (1994). Targeted and natural (piebald-lethal) mutations of endothelin-B receptor gene produce megacolon associated with spotted coat color in mice. Cell, 79(7):1267–1276. doi: 10.1016/0092-8674(94)90017-5. [PubMed: 8001159]
14. Milla PJ (1999). Endothelins, pseudo-obstruction and Hirschsprung's disease. Gut, 44(2):148–149. doi: 10.1136/gut.44.2.148. [PubMed: 9895366]
15. Edery P, Attié T, Amiel J, Pelet A, Eng C, Hofstra RM, Martelli H, Bidaud C, Munnich A, Lyonnet S. (1996). Mutation of the endothelin-3 gene in the Waardenburg-Hirschsprung disease (Shah-Waardenburg syndrome). Nat Genet, 12(4):442–444. doi: 10.1038/ng0496-442. [PubMed: 8630502]
16. Hofstra RM, Osinga J, Tan-Sindhunata G, Wu Y, Kamsteeg EJ, Stulp RP, van Ravenswaaij-Arts C, Majoor-Krakauer D, Angrist M, Chakravarti A, Meijers C, Buys CH (1996). A homozygous mutation in the endothelin-3 gene associated with a combined Waardenburg type

2 and Hirschsprung phenotype (Shah-Waardenburg syndrome). Nat Genet, 12(4):445–457. doi: 10.1038/ng0496-445. [PubMed: 8630503]

17. Kusafuka T, Wang Y, Puri P. (1996). Novel mutations of the endothelin-B receptor gene in isolated patients with Hirschsprung's disease. Hum Mol Genet. 5(3):347–349. doi: 10.1093/hmg/5.3.347. [PubMed: 8852658]
18. Puffenberger EG, Hosoda K, Washington SS, Nakao K, deWit D, Yanagisawa M, Chakravart A. (1994). A missense mutation of the endothelin-B receptor gene in multigenic Hirschsprung's disease. Cell, 30;79(7):1257–1266. doi: 10.1016/0092-8674(94)90016-7 [PubMed: 8001158]
19. Lin WW, Lee CY (1992). Intestinal relaxation by endothelin isopeptides: involvement of Ca(2+)-activated K+ channels. Eur J Pharmacol, 219(3):355–360. doi: 10.1016/0014-2999(92)90475-j. [PubMed: 1425964]
20. Yoshimura M, Yamashita Y, Kan S, Niwa M, Taniyama K. (1996). Localization of endothelin ETB receptors on the myenteric plexus of guinea-pig ileum and the receptor-mediated release of acetylcholine. Br J Pharmacol, 118(5):1171–1176. doi: 10.1111/j.1476-5381.1996.tb15520.x. [PubMed: 8818340]
21. Peters CM, Rogers SD, Pomonis JD, Egnaczyk GF, Keyser CP, Schmidt JA, Ghilardi JR, Maggio JE, Mantyh PW. (2003). Endothelin receptor expression in the normal and injured spinal cord: potential involvement in injury-induced ischemia and gliosis. Exp Neurol, 180(1):1–13. doi: 10.1016/s0014-4886(02)00023-7. [PubMed: 12668144]
22. Mule NK, Singh JN, Shah KU, Gulati A, Sharma SS (2018). Endothelin-1 Decreases Excitability of the Dorsal Root Ganglion Neurons via ET B Receptor. Mol Neurobiol, 55(5):4297–4310. doi: 10.1007/s12035-017-0640-1. [PubMed: 28623618]
23. Yamamoto T, Ono K, Hitomi S, Harano N, Sago T, Yoshida M, Nunomaki M, Shiiba S, Watanabe S, Nakanishi O, Inenaga K. (2013). Endothelin receptor-mediated responses in trigeminal ganglion neurons. J Dent Res, 92(4):335–339. doi: 10.1177/0022034513478428. [PubMed: 23396520]
24. Gulbransen BD, Christofi FL (2018). Are We Close to Targeting Enteric Glia in Gastrointestinal Diseases and Motility Disorders? Gastroenterology,155(2):245–251. doi: 10.1053/j.gastro.2018.06.050. [PubMed: 29964042]
25. Grubišić V, Gulbransen BD (2017). Enteric glial activity regulates secretomotor function in the mouse colon but does not acutely affect gut permeability. J Physiol, 595(11):3409–3424. doi: 10.1113/JP273492. [PubMed: 28066889]
26. MacEachern SJ, Patel BA, Keenan CM, Dicay M, Chapman K, McCafferty DM, Savidge TC, Beck PL, MacNaughton WK, Sharkey KA (2015). Inhibiting Inducible Nitric Oxide Synthase in Enteric Glia Restores Electrogenic Ion Transport in Mice With Colitis. Gastroenterology, 149(2):445–455.e3. doi: 10.1053/j.gastro.2015.04.007. [PubMed: 25865048]
27. Murch SH, Braegger CP, Sessa WC, MacDonald TT (1992). High endothelin-1 immunoreactivity in Crohn's disease and ulcerative colitis. Lancet, 339(8790):381–385. doi: 10.1016/0140-6736(92)90077-g. [PubMed: 1346658]
28. McClain J, Grubišić V, Fried D, Gomez-Suarez RA, Leinninger GM, Sévigny J, Parpura V, Gulbransen BD (2014). Ca^{2+} responses in enteric glia are mediated by connexin-43 hemichannels and modulate colonic transit in mice. Gastroenterology, 146(2):497–507.e1. doi: 10.1053/j.gastro.2013.10.061. [PubMed: 24211490]
29. Ahmadzai MM, Seguella L, Gulbransen BD (2021). Circuit-specific enteric glia regulate intestinal motor neurocircuits. Proc Natl Acad Sci U S A, 118(40):e2025938118. doi: 10.1073/pnas.2025938118.
30. Delvalle NM, Fried DE, Rivera-Lopez G, Gaudette L, Gulbransen BD (2018). Cholinergic activation of enteric glia is a physiological mechanism that contributes to the regulation of gastrointestinal motility. Am J Physiol Gastrointest Liver Physiol. 315(4):G473–G483. doi: 10.1152/ajpgi.00155.2018. [PubMed: 29927320]
31. McClain JL, Fried DE, Gulbransen BD (2015). Agonist-evoked Ca2+ signaling in enteric glia drives neural programs that regulate intestinal motility in mice. Cell Mol Gastroenterol Hepatol. 1(6):631–645. doi: 10.1016/j.jcmgh.2015.08.004. [PubMed: 26693173]

32. Seguella L, Gulbransen BD (2021). Enteric glial biology, intercellular signalling and roles in gastrointestinal disease. Nat Rev Gastroenterol Hepatol.18(8):571–587. doi: 10.1038/s41575-021-00423-7. [PubMed: 33731961]
33. Mazzotta E, Villalobos-Hernandez EC, Fiorda-Diaz J, Harzman A, Christofi FL (2020). Postoperative Ileus and Postoperative Gastrointestinal Tract Dysfunction: Pathogenic Mechanisms and Novel Treatment Strategies Beyond Colorectal Enhanced Recovery After Surgery Protocols. Front Pharmacol, 11:583422. doi: 10.3389/fphar.2020.583422.
34. Ochoa-Cortes F, Turco F, Linan-Rico A, Soghomonyan S, Whitaker E, Wehner S, Cuomo R, Christofi FL (2016). Enteric Glial Cells: A New Frontier in Neurogastroenterology and Clinical Target for Inflammatory Bowel Diseases. Inflamm Bowel Dis, 22(2):433–449. doi: 10.1097/MIB.0000000000000667. [PubMed: 26689598]
35. Schneider R, Leven P, Glowka T, Kuzmanov I, Lysson M, Schneiker B, Miesen A, Baqi Y, Spanier C, Grants I, Mazzotta E, Villalobos-Hernandez E, Kalff JC, Müller CE, Christofi FL, Wehner S. (2021). A novel P2X2-dependent purinergic mechanism of enteric gliosis in intestinal inflammation. EMBO Mol Med, 13(1):e12724. doi: 10.15252/emmm.202012724.
36. Schneider R, Leven P, Mallesh S, Breßer M, Schneider L, Mazzotta E, Fadda P, Glowka T, Vilz TO, Lingohr P, Kalff JC, Christofi FL, Wehner S. (2022). IL-1-dependent enteric gliosis guides intestinal inflammation and dysmotility and modulates macrophage function. Commun Biol, 5(1):811. doi: 10.1038/s42003-022-03772-4. [PubMed: 35962064]
37. Stoffels B, Hupa KJ, Snoek SA, van Bree S, Stein K, Schwandt T, Vilz TO, Lysson M, Veer CV, Kummer MP, Hornung V, Kalff JC, de Jonge WJ, Wehner S. (2014). Postoperative ileus involves interleukin-1 receptor signaling in enteric glia. Gastroenterology, 146(1):176–187.e1. doi: 10.1053/j.gastro.2013.09.030. [PubMed: 24067878]
38. Liñán-Rico A, Turco F, Ochoa-Cortes F, Harzman A, Needleman BJ, Arsenescu R, Abdel-Rasoul M, Fadda P, Grants I, Whitaker E, Cuomo R, Christofi FL (2016). Molecular Signaling and Dysfunction of the Human Reactive Enteric Glial Cell Phenotype: Implications for GI Infection, IBD, POI, Neurological, Motility, and GI Disorders. Inflamm Bowel Dis, 22(8):1812–1934. doi: 10.1097/MIB.0000000000000854. [PubMed: 27416040]
39. McClain JL, Mazzotta EA, Maradiaga N, Duque-Wilckens N, Grants I, Robison AJ, Christofi FL, Moeser AJ, Gulbransen BD (2020). Histamine-dependent interactions between mast cells, glia, and neurons are altered following early-life adversity in mice and humans. Am J Physiol Gastrointest Liver Physiol, 319(6):G655–G668. doi: 10.1152/ajpgi.00041.2020. [PubMed: 32996781]
40. Gulbransen BD, Bashashati M, Hirota SA, Gui X, Roberts JA, MacDonald JA, Muruve DA, McKay DM, Beck PL, Mawe GM, Thompson RJ, Sharkey KA (2012). Activation of neuronal P2X7 receptor-pannexin-1 mediates death of enteric neurons during colitis. Nat Med,18(4):600–604. doi: 10.1038/nm.2679. [PubMed: 22426419]
41. Fujikawa Y, Tominaga K, Tanaka F, Tanigawa T, Watanabe T, Fujiwara Y, Arakawa T. (2015). Enteric glial cells are associated with stress-induced colonic hyper-contraction in maternally separated rats. Neurogastroenterol Motil, 27(7):1010–1023. doi: 10.1111/nmo.12577. [PubMed: 25960044]
42. Lilli NL, Quénéhervé L, Haddara S, Brochard C, Aubert P, Rolli-Derkinderen M, Durand T, Naveilhan P, Hardouin J-B., De Giorgio R, Barbara G, Bruley des Varannes S, Coron E, Neunlist M. (2018). Glioplasticity in irritable bowel syndrome. Neurogastroenterol Motil, 30(4):e13232. doi: 10.1111/nmo.13232.
43. Laranjeira C, Sandgren K, Kessaris N, Richardson W, Potocnik A, Vanden Berghe P, Pachnis V. (2011). Glial cells in the mouse enteric nervous system can undergo neurogenesis in response to injury. J Clin Invest, 121(9):3412–3424. doi: 10.1172/JCI58200. [PubMed: 21865647]
44. LeComte MD, Shimada IS, Sherwin C, Spees JL (2015). Notch1-STAT3-ETBR signaling axis controls reactive astrocyte proliferation after brain injury. Proc Natl Acad Sci U S A, 112(28):8726–8731. doi: 10.1073/pnas.1501029112. [PubMed: 26124113]
45. Rogers SD, Peters CM, Pomonis JD, Hagiwara H, Ghilardi JR, Mantyh PW (2003). Endothelin B receptors are expressed by astrocytes and regulate astrocyte hypertrophy in the normal and injured CNS. Glia, 41(2):180–190. doi: 10.1002/glia.10173. [PubMed: 12509808]

46. Gong S, Zheng C, Doughty ML, Losos K, Didkovsky N, Schambra UB, Nowak NJ, Joyner A, Leblanc G, Hatten ME, Heintz N. (2003). A gene expression atlas of the central nervous system based on bacterial artificial chromosomes. Nature, 425(6961):917–925. doi: 10.1038/nature02033. [PubMed: 14586460]
47. Linan-Rico A, Grants I, Needleman BJ, Williams KC, Soghomonyan S, Turco F, Cuomo R, Grider JR, Kendig DM, Murthy KS, Harzman A, Ochoa-Cortes F, Christofi FL (2015). Gliomodulation of Neuronal and Motor Behavior in the Human GI Tract. Gastroenterology, 148(4):S-18, doi:10.1016/S0016-5085(15)30063-9.
48. Gee JM, Smith NA, Fernandez FR, Economo MN, Brunert D, Rothermel M, Morris SC, Talbot A, Palumbos S, Ichida JM, Shepherd JD, West PJ, Wachowiak M, Capecchi MR, Wilcox KS, White JA, Tvrdik P. (2014). Imaging activity in neurons and glia with a Polr2a-based and cre-dependent GCaMP5G-IRES-tdTomato reporter mouse. Neuron 83, 1058–1072. 10.1016/j.neuron.2014.07.024 [PubMed: 25155958]
49. McClain JL, Gulbransen BD (2017). The acute inhibition of enteric glial metabolism with fluoroacetate alters calcium signaling, hemichannel function, and the expression of key proteins. J Neurophysiol, 117(1):365–375. doi: 10.1152/jn.00507.2016. [PubMed: 27784805]
50. Grubišić V, McClain JL, Fried DE, Grants I, Rajasekhar P, Csizmadia E, Ajijola OA, Watson RE, Poole DP, Robson SC, Christofi FL, Gulbransen BD (2020). Enteric Glia Modulate Macrophage Phenotype and Visceral Sensitivity following Inflammation. Cell Rep, 32(10):108100. doi: 10.1016/j.celrep.2020.108100.
51. Grundmann D, Klotz M, Rabe H, Glanemann M, Schäfer KH (2015). Isolation of high-purity myenteric plexus from adult human and mouse gastrointestinal tract. Sci Rep, 5:9226. doi: 10.1038/srep09226. [PubMed: 25791532]
52. Mallesh S, Schneider R, Schneiker B, Lysson M, Efferz P, Lin E, de Jonge WJ, Wehner S. (2021). Sympathetic Denervation Alters the Inflammatory Response of Resident Muscularis Macrophages upon Surgical Trauma and Ameliorates Postoperative Ileus in Mice. Int J Mol Sci, 22(13): 6872. doi: 10.3390/ijms22136872. [PubMed: 34206766]
53. Ren T, Grants I, Alhaj M, McKiernan M, Jacobson M, Hassanain HH, Frankel W, Wunderlich J, Christofi FL (2011). Impact of disrupting adenosine A_3 receptors ($A_3^{-/-}$ AR) on colonic motility or progression of colitis in the mouse. Inflamm Bowel Dis, 17(8):1698–713. doi: 10.1002/ibd.21553. [PubMed: 21744424]
54. Kendig DM, Hurst NR, Grider JR (2016). Spatiotemporal Mapping of Motility in Ex Vivo Preparations of the Intestines, JOVE, Jan 27(107):e53263. doi: 10.3791/53263.
55. Leven P, Schneider R, Siemens KD, Jackson WS, Wehner S. (2022). Application of a RiboTag-based approach to generate and analyze mRNA from enteric neural cells. Neurogastroenterol Motil, 34(7):e14309. doi: 10.1111/nmo.14309.
56. Gulbransen BD, Sharkey KA (2009). Purinergic neuron-to-glia signaling in the enteric nervous system. Gastroenterology, 136(4):1349–1358. doi: 10.1053/j.gastro.2008.12.058. [PubMed: 19250649]
57. Khodorova A, Zou S, Ren K, Dubner R, Davar G, Strichartz G. Dual Roles for Endothelin-B Receptors in Modulating Adjuvant-Induced Inflammatory Hyperalgesia in Rats. Open Pain J. 2009;2:30–40. doi: 10.2174/1876386300902010030. [PubMed: 20559459]
58. Ługowska-Umer H, Umer A, Kuziemski K, Sein-Anand Ł, Korolkiewicz RP. (2019). The protective effect of endothelin receptor antagonists against surgically induced impairment of gastrointestinal motility in rats. J Smooth Muscle Res, 55(0):23–33. doi: 10.1540/jsmr.55.23. [PubMed: 31527357]
59. Yoshinaga M, Chijiiwa Y, Misawa T, Harada N, Nawata H. (1992). Endothelin B receptor on guinea pig small intestinal smooth muscle cells. Am J Physiol, 262(2 Pt 1):G308-G311. doi: 10.1152/ajpgi.1992.262.2.G308.
60. Soboleski MR, Oaks J, Halford WP (2005). Green fluorescent protein is a quantitative reporter of gene expression in individual eukaryotic cells. FASEB J, 19(3):440–442. doi: 10.1096/fj.04-3180fje. [PubMed: 15640280]
61. Snapp E. (2005). Design and use of fluorescent fusion proteins in cell biology. Curr Protoc Cell Biol, 27(1):21.4.1–21.4.13. doi: 10.1002/0471143030.cb2104s27.

62. Q LV, Guo K, Xu H, Wang T, Zhang Y. (2015). Identification of Putative ORF5 Protein of Porcine Circovirus Type 2 and Functional Analysis of GFP-Fused ORF5 Protein. PLoS One. 10(6):e0127859. doi: 10.1371/journal.pone.0127859.

63. Feldman-Goriachnik R, Hanani M. (2011). Functional study of endothelin B receptors in satellite glial cells in trigeminal ganglia. Neuroreport, 22(10):465–469. doi: 10.1097/WNR.0b013e3283472487. [PubMed: 21642881]

64. Milner P, Loesch A, Burnstock G. (2000). Endothelin immunoreactivity and mRNA expression in sensory and sympathetic neurones following selective denervation. Int J Dev Neurosci. 18(8):727–734. doi: 10.1016/s0736-5748(00)00054-x. [PubMed: 11154842]

65. Lee PR, Fields RR (2021). Activity-Dependent Gene Expression in Neurons. Neuroscientist, 27(4):355–366. doi: 10.1177/1073858420943515. [PubMed: 32727285]

66. Brosenitsch TA, Katz DM (2001). Physiological patterns of electrical stimulation can induce neuronal gene expression by activating N-type calcium channels. J Neurosci, 21(8):2571–2579. doi: 10.1523/JNEUROSCI.21-08-02571.2001. [PubMed: 11306610]

67. LeMasson G, Marder E, Abbott LF (1993). Activity-dependent regulation of conductances in model neurons. Science, 259(5103):1915–1917. doi: 10.1126/science.8456317. [PubMed: 8456317]

68. Barr TP, Kornberg D, Montmayeur J-P, Long M, Reichheld S, Strichartz GR (2015). Validation of endothelin B receptor antibodies reveals two distinct receptor-related bands on Western blot. Anal Biochem, 468:28–33. doi: 10.1016/j.ab.2014.09.004. [PubMed: 25232999]

69. Boyd R, Rätsep MT, Ding LL, Wang HD (2011) ETA and ETB receptors are expressed in vascular adventitial fibroblasts. Am J Physiol Heart Circ Physiol, 301(6):H2271–H2278. doi: 10.1152/ajpheart.00869.2010. [PubMed: 21949113]

70. Islamov RR, Chintalgattu V, McMurray RJ, Pak ES, Murashov AK, Katwa LC (2003). Differential expression of endothelin receptors in regenerating spinal motor neurons in mice. Brain Res Mol Brain Res, 116(1–2):163–167. doi: 10.1016/s0169-328x(03)00258-4. [PubMed: 12941473]

71. Quaschning T, Voss F, Relle K, Kalk P, Vignon-Zellweger N, Pfab T, Bauer C, Theilig F, Bachmann S, Kraemer-Guth A, Wanner C, Theuring F, Galle J, Hocher B. (2007). Lack of endothelial nitric oxide synthase promotes endothelin-induced hypertension: lessons from endothelin-1 transgenic/endothelial nitric oxide synthase knockout mice. J Am Soc Nephrol, 18(3):730–740. doi: 10.1681/ASN.2006050541. [PubMed: 17287431]

72. De Schepper HU, De Winter BY, Seerden TC, Herman AG, Pelckmans PA, De Man JG (2005). Functional characterisation of tachykinin receptors in the circular muscle layer of the mouse ileum. Regul Pept, 130(3):105–115. doi: 10.1016/j.regpep.2005.04.003. [PubMed: 15935491]

73. Gardner A, Westfall TC, Macarthur H. (2005). Endothelin (ET)-1-induced inhibition of ATP release from PC-12 cells is mediated by the ETB receptor: differential response to ET-1 on ATP, neuropeptide Y, and dopamine levels. J Pharmacol Exp Ther, 313(3):1109–1117. doi: 10.1124/jpet.104.081075. [PubMed: 15687374]

74. Filosa JA, Naskar K, Perfume G, Iddings JA, Biancardi V.c., Vatta M.s., Stern JE (2012). Endothelin-mediated calcium responses in supraoptic nucleus astrocytes influence magnocellular neurosecretory firing activity. J Neuroendocrinol, 24(2):378–392. doi: 10.1111/j.1365-2826.2011.02243.x. [PubMed: 22007724]

75. Rao M, Rastelli D, Dong L, Chiu S, Setlik W, Gershon MD, Corfas G. (2017). Enteric Glia Regulate Gastrointestinal Motility but Are Not Required for Maintenance of the Epithelium in Mice. Gastroenterology, 153(4):1068–1081.e7. doi: 10.1053/j.gastro.2017.07.002. [PubMed: 28711628]

76. Nasser Y, Fernandez E, Keenan CM, Ho W, Oland LD, Tibbles LA, Schemann M, MacNaughton WK, Rühl A, Sharkey KA (2006). Role of enteric glia in intestinal physiology: effects of the gliotoxin fluorocitrate on motor and secretory function. Am J Physiol Gastrointest Liver Physiol, 291(5):G912–27. doi: 10.1152/ajpgi.00067.2006. [PubMed: 16798727]

77. Gariepy CE, Cass DT, Yanagisawa M. (1996). Null mutation of endothelin receptor type B gene in spotting lethal rats causes aganglionic megacolon and white coat color. Proc Natl Acad Sci U S A, 93(2):867–872. doi: 10.1073/pnas.93.2.867. [PubMed: 8570650]

78. Giller T, Breu V, Valdenaire O, Clozel M. (1997). Absence of ET(B)-mediated contraction in Piebald-lethal mice. Life Sci, 61(3):255–263. doi: 10.1016/s0024-3205(97)00381-0. [PubMed: 9217285]

79. Alexander SPH, et al. (2021). The Concise Guide to PHARMACOLOGY 2021/22: G-protein coupled receptors. Br J Pharmacol, 178: S27–S156. [PubMed: 34529832]

80. Alexander SPH et al. (2018). Goals and practicalities of immunoblotting and immunohistochemistry: A guide for submission to the British Journal of Pharmacology. Br J Pharmacol. 175(3):407–411. doi: 10.1111/bph.14112. [PubMed: 29350411]

81. Curtis MJ et al. , (2018). Experimental design and analysis and their reporting II: updated and simplified guidance for authors and peer reviewers. Br J Pharmacol. 175(7):987–993. doi: 10.1111/bph.14153. [PubMed: 29520785]

Summary:

What is already known:

- Endothelin may interact with ETA_R and ETB_R to modulate motility, but the role of ETB_R is unclear
- Endothelin signaling is implicated in tissue inflammation, neurological diseases, pulmonary hypertension, sepsis, pancreatitis, IBD, and necrotizing enterocolitis

What this study adds:

- Enteric glial ET-1/ETB_R signaling provides modulation of two distinct enteric neural-motor pathways to inhibit motility
- Glial ETB_R signaling is linked to intestinal inflammation in a postoperative ileus model

Clinical Significance:

- Enteric glial ETB_R is a potential novel pharmacological target for intestinal motility disorders
- Amplification of glial ETB_R is linked to *muscularis externa* inflammation and pathogenic mechanisms of postoperative ileus

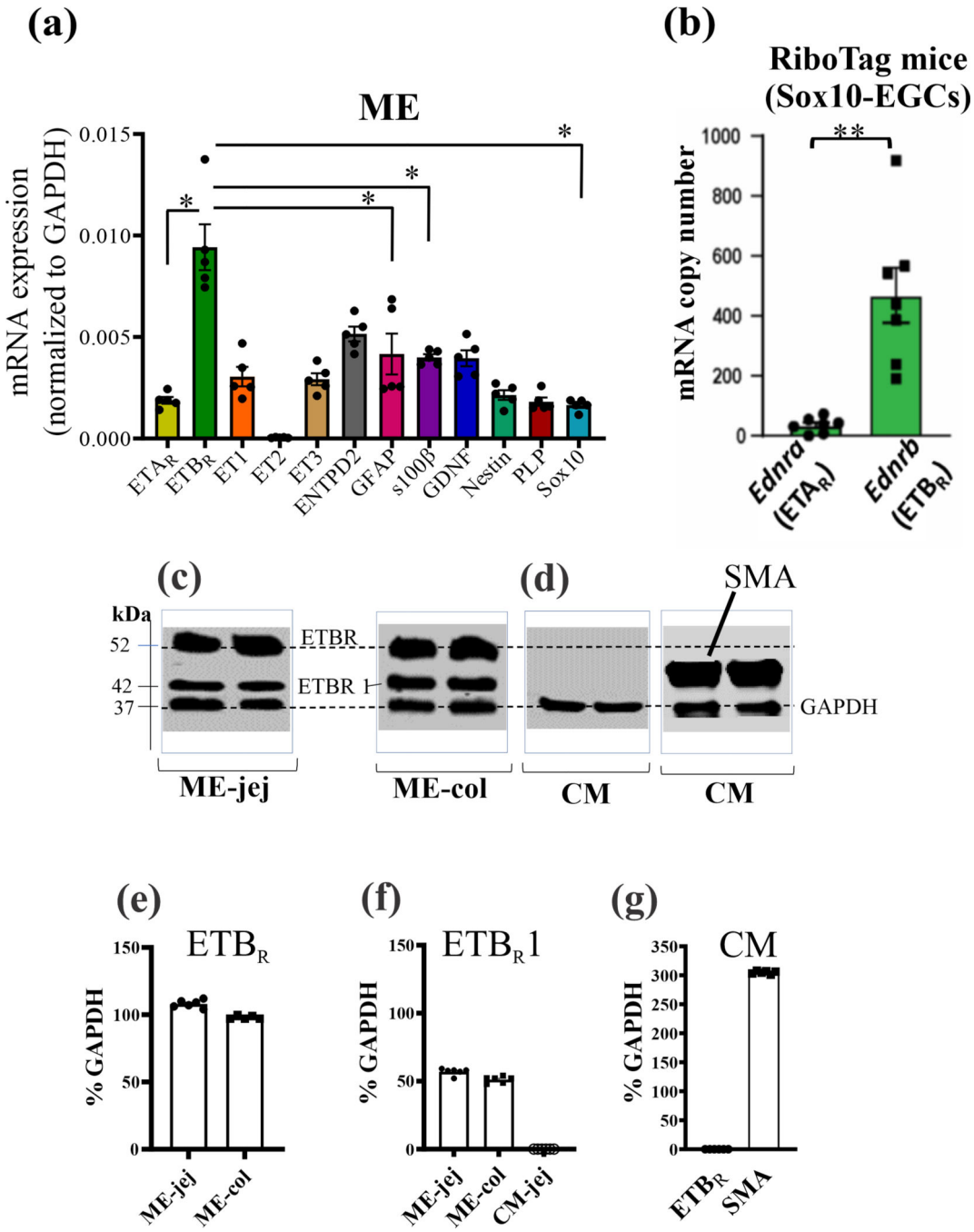

Figure 1. Expression of ETB_R in muscularis externa (ME) of wild-type mice and glia of RiboTag (Sox10-EGCs) mice.

(a) Quantitative PCR analysis identified mRNA transcripts in ME of wild-type mice for ETB_R, ETA_R, ET1, ET3, ENTPD2, GFAP, s100β, GDNF, Nestin, PLP and Sox10; n=5 mice; differences between groups are significant at *p<0.01. Note: ETB_R expression >> ETA_R expression. For Fig. 2a, one-way ANOVA, followed by multiple comparisons using Tukey's test, *p<0.01. (b) In RiboTag (Sox10-EGCs) mice, mRNA levels for ETB_R >> ETA_R (**p<0.001) (c) Protein expression of ETB_R reveals 2 immunogenic bands at ~52kDa and 42kDa (ETB_R1, arbitrary label) in the ME of jejunum or colon. (d) In CM, ETB_R

protein is not expressed; α-smooth muscle actin (SMA) is highly expressed in the CM of the same lysate samples. (e) Quantitative analysis of ETB_R protein in ME. (f) ETB_R1 is expressed in ME but not CM. (g) ETB_R is not expressed in CM identified by α-SMA; n=6 mice.

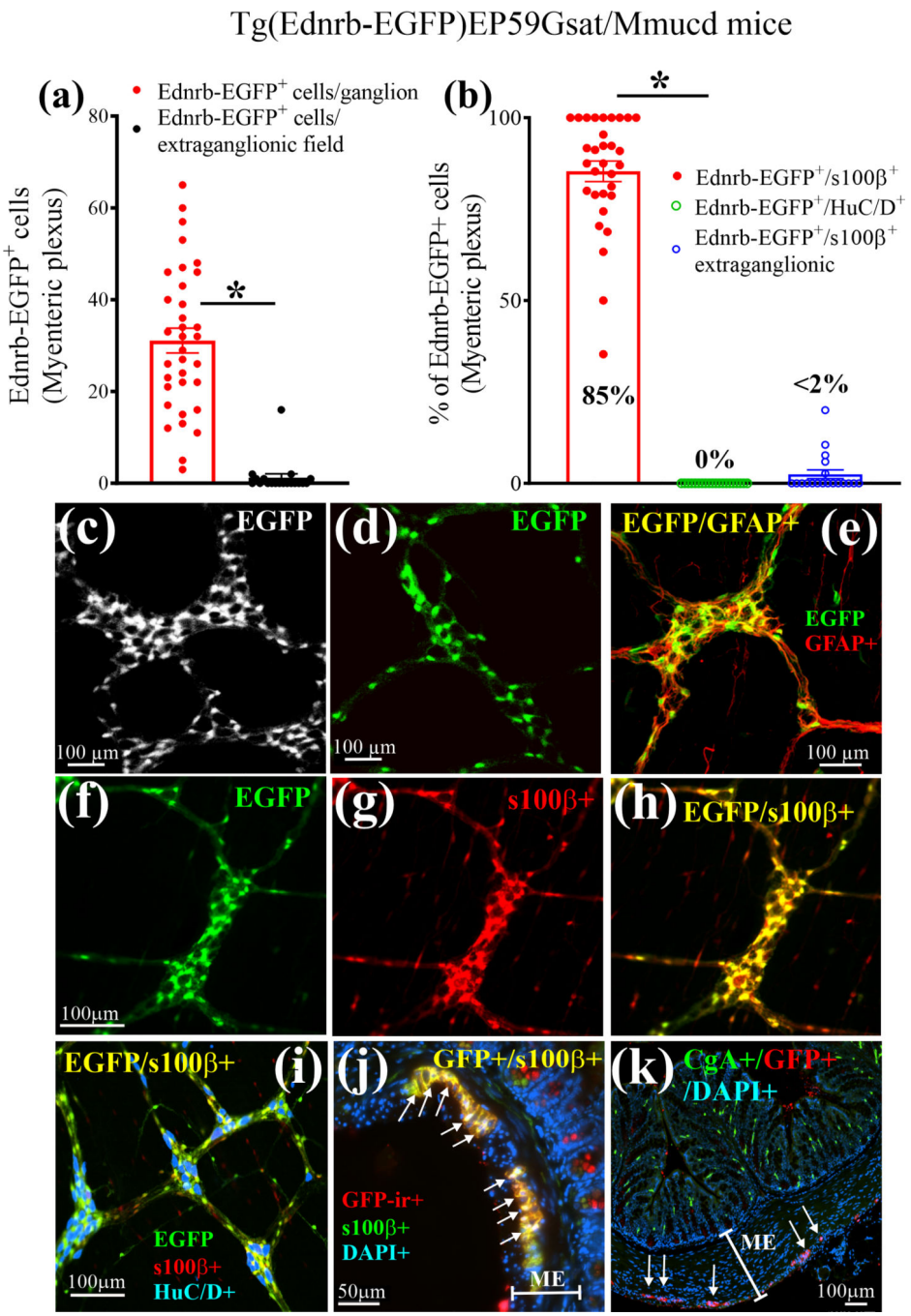

Figure 2. Cellular expression and distribution of EGFP reporter protein in the intestinal tract of Tg(Ednrb-EGFP)EP59Gsat/Mmucd ETB_R mice.

(a) EGFP is expressed in myenteric ganglia and is absent in extra-ganglionic cells of the ME in intact LMMP-CM preparations. (b) EGFP reporter is exclusively expressed in glia ($s100\beta^+$ cells) and is absent from neurons (HuC/D^+ cells) in myenteric ganglia of the ME; for a and b, n=35 image fields (5 image fields/animal and counts of all EGFP cells; n=7 animals) (c) Black and white LSM image of ETB_R^+ glial cells in myenteric ganglia visualized by EGFP expression. (d) Another LSM image of ETB_R^+ glial cells in myenteric ganglia visualized by EGFP. (e) Co-localization of ETB_R^+ cells (green) with the glial

marker GFAP (red); yellow denotes colocalization. (f-h) Co-localization of ETB_R^+ cells with the glial marker s100β; (f) image of ETB_R^+(EGFP) cells; (g) image of $s100\beta^+$ glia; (h) overlay image for co-labeling of EGFP and $s100\beta^+$ cells. (i) ETB_R (green) is co-localized in $s100\beta^+$glia (red) but not neurons (blue, HuC/D); co-localized cells in the overlay image are yellow. (j) GFP-immunoreactivity (ir) in de-paraffinized cross-sections of the colon (10μm sections, 3-D z-stack constructed at 0.5μm sections) is highly expressed in $s100^+$glia and a few cells in the mucosa. (k) GFP-ir is not expressed in CgA^+ enteroendocrine cells of the mucosa, but is expressed in myenteric ganglia (arrows) of the ME.

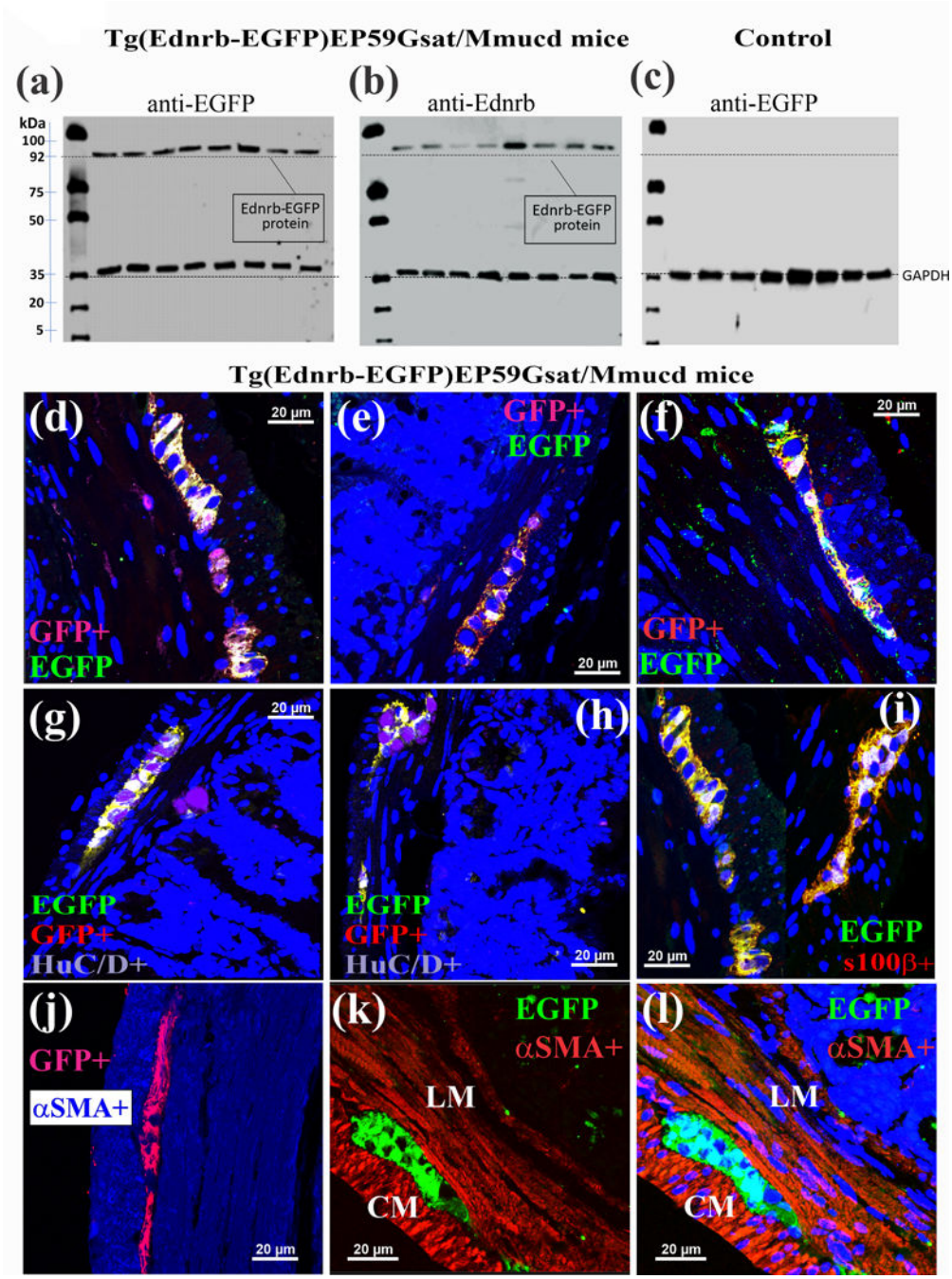

Figure 3. Ednrb (ETB_R) expression in glia is revealed in LMMP-CM preparations from Tg (Ednrb-EGFP) EP59Gsat/Mmucd mice.

(a-b) Western blot analysis identified a protein with a molecular weight ~90kDa in Tg mice that was recognized by (a) an anti-EGFP antibody or (b) an anti-Ednrb antibody in lysates of jejunum *muscularis externa*. (c) In a control animal (wild type), EGFP is not expressed. (d-f) GFP (EGFP)-immunoreactivity is co-localized with the EGFP reporter protein. (g,h) GFP-immunoreactivity is not co-localized with HuC/D^+ neurons. (i) GFP-immunoreactivity is co-localized with $s100\beta^+$glia. (i-l) GFP-immunoreactivity is not co-localized with αSMA in smooth muscle layers. Z-stack images were captured by laser confocal imaging of GFP-

immunoreactivity (ir) in de-paraffinized cross-sections of the colon (10μm sections, 0.5μm sections were used for z-stack analysis).

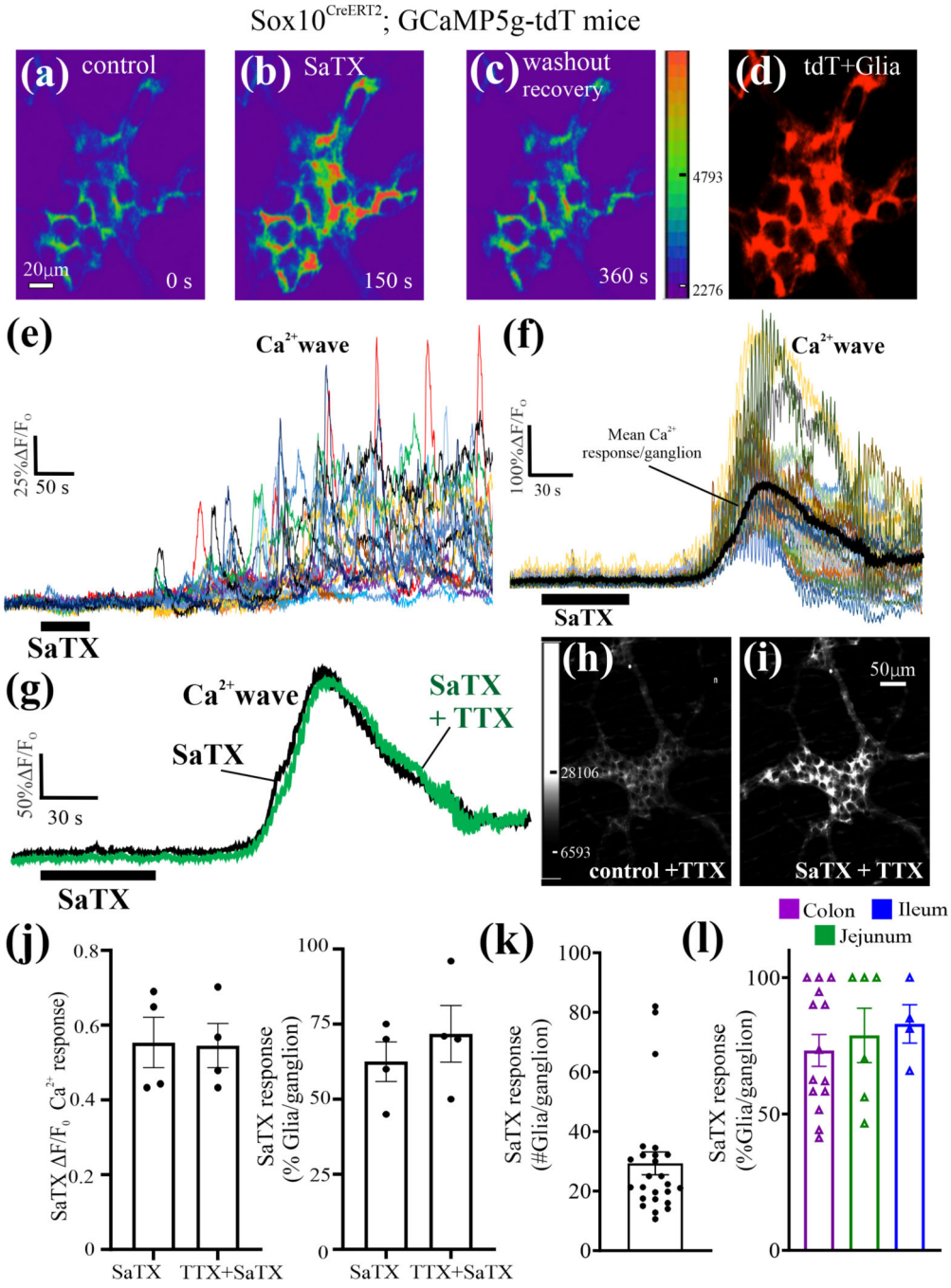

Figure 4. SaTX triggers a glial Ca^{2+} wave in intact myenteric plexus preparations (LMMP).
(a-d) The selective ETB_R agonist SaTX (50nM) triggers a Ca^{2+} response in glia; pseudocolor images according to intensity of Ca^{2+} response; glia are identified by tdT^+cells (d). (e) The Ca^{2+} wave response to SaTX in the ganglion shown in images 'a-d' represents individual Ca^{2+}transients occurring in each tdT^+ glia. (f) Another example of a Ca^{2+} wave in a different ganglion. Note: the mean Ca^{2+} response obtained by averaging all the Ca^{2+} transients in each ganglion is shown, and it is used for quantitative analysis of the mean Ca^{2+} response/ganglion. (g-i) The Ca^{2+} response induced by 50nM SaTX persists in the presence

of 1μM TTX; (g) the mean Ca^{2+} response to SaTX in a myenteric ganglion is shown before and after a 10 min perfusion of TTX; (h,i) images showing that the SaTX response in a ganglion still occurs after TTX treatment of the ganglion. (j) The Ca^{2+} response to SaTX does not appear to be sensitive to TTX treatment. (k) Number of glia/myenteric ganglion responding to SaTX with a Ca^{2+} wave in jejunum. (l) SaTX Ca^{2+} responses occur in glia of the myenteric plexus of the ileum, jejunum and colon. Ca^{2+}imaging was done using $Sox10^{CreERT2}$;GCaMP5g-tdT mice.

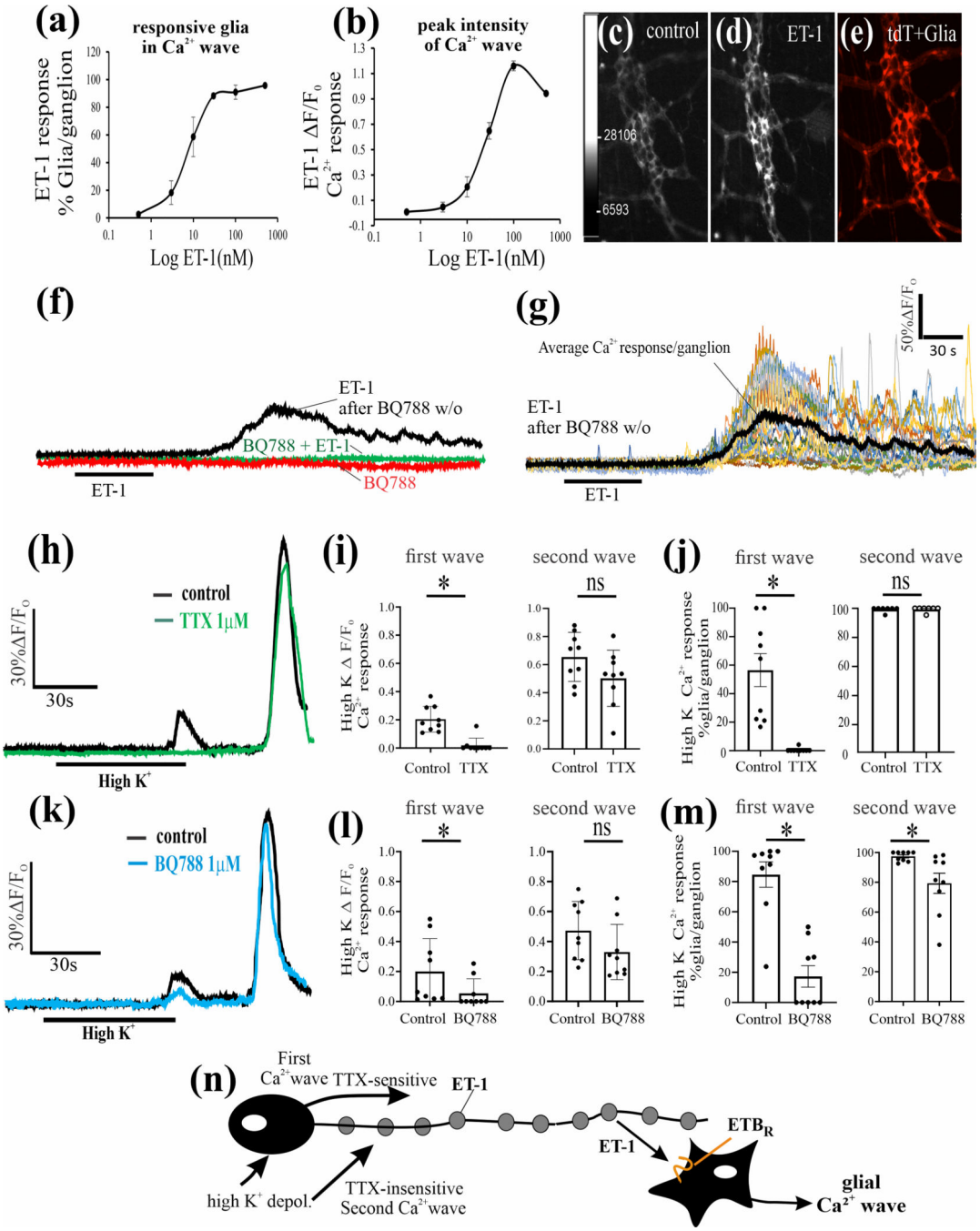

Figure 5. Endothelin (ET-1) activates ETB_R signaling in enteric glia from $Sox10^{CreERT2}$;GCaMP5g-tdT mice.

(a-b). Exogenous ET-1 triggers a concentration–dependent Ca^{2+}response in glia. (c-e) Pseudocolor images showing an example of a control baseline Ca^{2+}response in the absence of ET-1 and the peak response to 50nM ET-1 in tdT^+ glia; concentration-response curves, n=5, one-way ANOVA, $p<0.01$. (f) The selective ETB_R antagonist BQ788 (1μM) blocks the Ca^{2+}wave triggered by 50nM ET-1. BQ788 alone has no effect on baseline Ca^{2+}responses. After exposure to BQ788 (30 min superfusion), ET-1 does not trigger a Ca^{2+}response. Washout of BQ788 by switching to Kreb's buffer perfusion for 20 min, and re-exposure to

ET-1 triggers a Ca^{2+}response; the Ca^{2+} response in ‘f’ represents the average response in all glia in the ganglion (referred to as mean Ca^{2+}response/ganglion). (g) Response to ET-1 after BQ788 washout in ‘f’ shown for individual glial Ca^{2+}transients in the Ca^{2+}wave used to generate the mean Ca^{2+} response for the ganglion. (h-j) High K^+ depolarization (75mM) of neurons triggers two different Ca^{2+}waves/responses separated by time. (h) The individual glial Ca^{2+} responses in each ganglion were averaged as shown in ‘h’ for analysis of data in different ganglia for effects of TTX. The first Ca^{2+}wave response is blocked by TTX whereas the second wave response is not sensitive to TTX as shown for a single ganglion (‘h’) and for pooled data (‘i, j’). (k) The Ca^{2+} wave responses in each ganglion were averaged as shown in ‘k’ for analysis of data in different ganglia for effects of BQ788. The ETB_R antagonist BQ788 blocks the first Ca^{2+}wave and reduces both the peak Ca^{2+}intensity and numbers of glia responding as shown for a single ganglion (‘k’) and for pooled data (‘l, m’). For the second Ca^{2+}wave, incubation pre-incubation with BQ788 causes a modest reduction only in the number of glia responding to high K^+ depolarization; for Figs 5i, j, l, m, *p<0.01; ns, not significant; n=9 separate ganglion experiments in LMMP preparations. (n) Our working model of high K^+ depolarization is illustrated, showing that activation of the cell soma of the neurons triggers a TTX-sensitive Ca^{2+}wave (involving Na_V-channels) involving the release of ET-1 from varicose nerve fibers in the ganglia (see Suppl. Fig. 2), whereas a delayed direct activation of varicose nerve fibers triggers a TTX-insensitive wave, although BQ788 could reduce the response. (*p<0.01; ns, not significant).

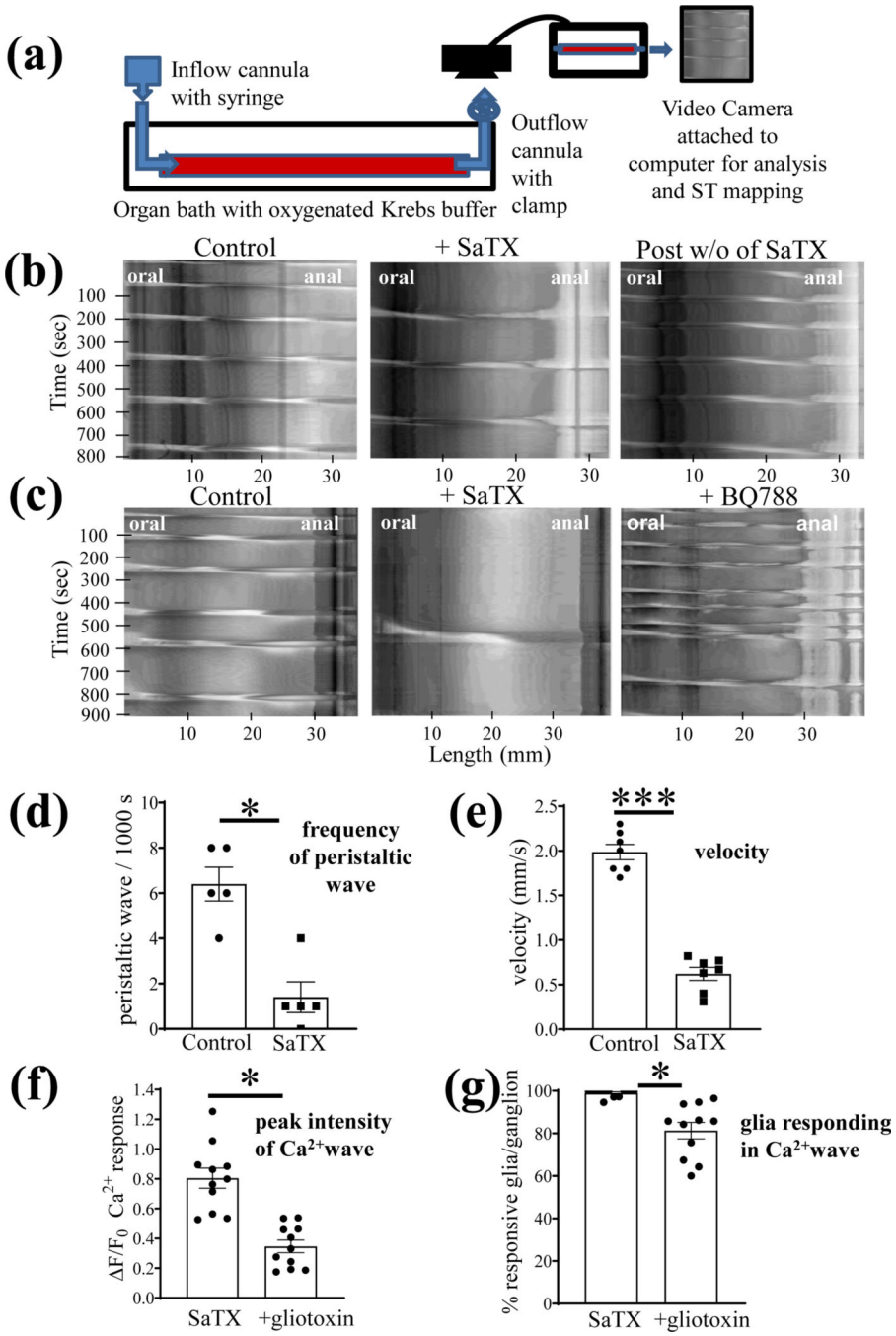

Figure 6. SaTX inhibits fluid induced peristaltic waves in the distal colon of the mouse.

(a) diagram showing the organ bath setup for elevating intraluminal fluid for spatiotemporal (ST) imaging of peristaltic waves. (b) representative example showing that SaTX (50 nM) can reversibly inhibit peristaltic waves induced by increasing pressure in the lumen with fluid. (c) SaTX has the opposite effect of BQ788 (1 μM) on fluid induced peristalsis. (d-e) SaTX inhibits both the frequency of the peristaltic wave and the velocity of propagation; (f-g) The gliotoxin fluoroacetate (90 min incubation, 0.1mM FA) partially reduces the magnitude of the Ca^{2+}response (i.e. ΔF/Fo) and the number of glia/ganglion responding in

the glial Ca^{2+}wave (%glia/ganglion) elicited by SaTX. For Fig. 6d-e, n=5 (or more) animals, *p<0.01, ***p<0.0001; For f and g, data represent the number of separate tissue experiments done in $Sox10^{CreERT2}$; GCaMP5g-tdT mice (n=11 different myenteric ganglia analyzed, *p<0.01). Data represents paired t-test analysis (with or without the intervention in the same preparations).

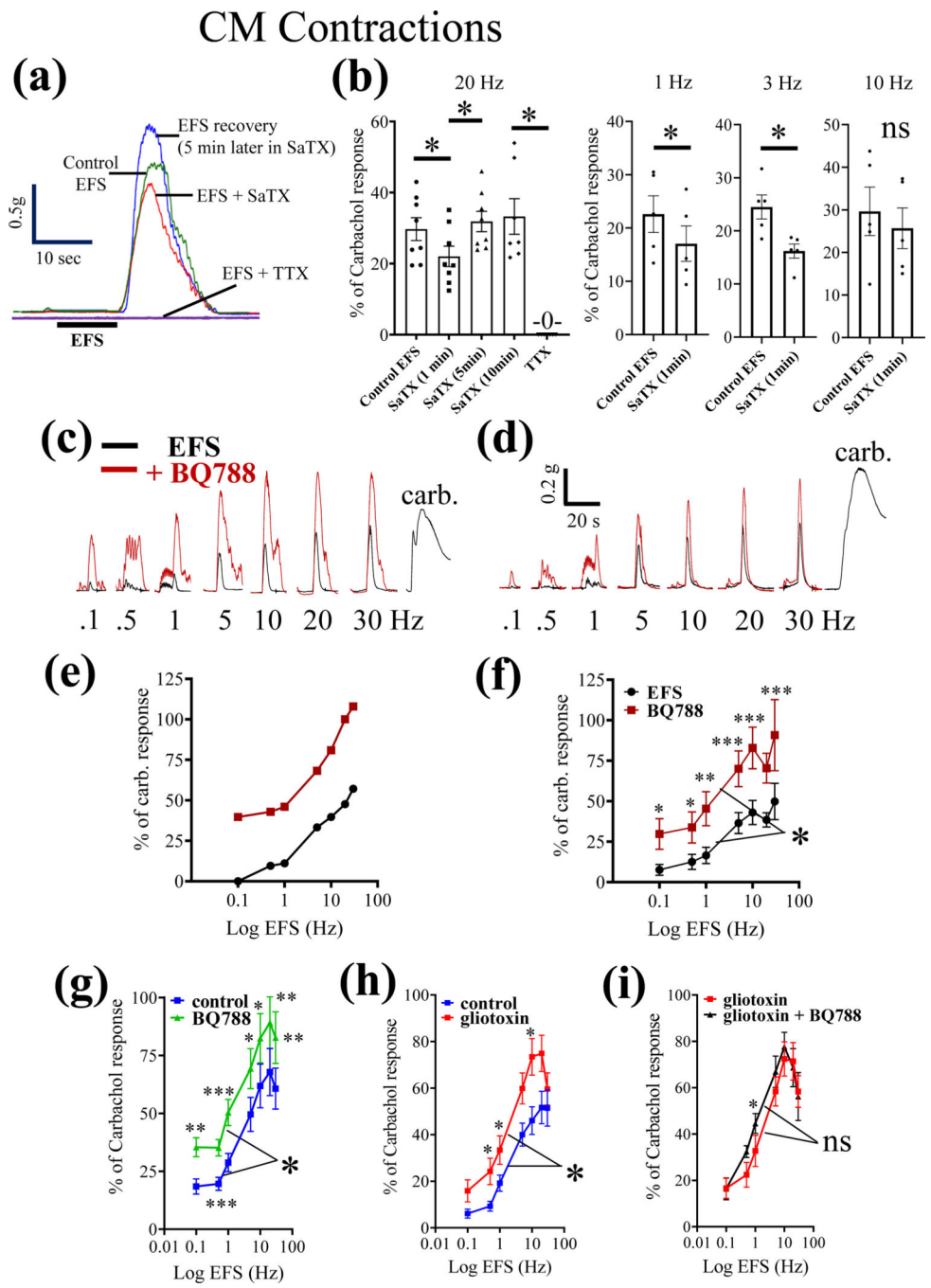

Figure 7. The physiological action of the selective ETB_R antagonist BQ788 is to enhance neuromuscular responses of the circular muscle (CM) to electrical field stimulation (EFS).

(a) Representative organ bath experiment showing that the EFS response is attenuated with 100nM SaTX at 20Hz, and the response fully recovers in the continued presence of SaTX. The response to EFS is abolished by blocking nerve conduction with 1 μM TTX. (b) Pooled data of the effects of SaTX on neuromuscular contractions induced by 20Hz EFS stimulation for data shown in (a). In separate experiments, SaTX is shown to inhibit 1Hz and 3Hz EFS stimulation. (c-d) two representative experiments showing the frequency-dependent effect of 3μM BQ788 EFS responses. (e-f) BQ788 significantly enhances the

frequency-dependent CM contractions to EFS; n=8 animals. 2-way ANOVA and post hoc analysis using Sidak's multiple comparison test, *p<0.01; **p<0.001; ***p<0.0001). (g-i) The influence of 3μM BQ788 on CM contractions is prevented by pretreatment with the gliotoxin FC (fluorocitrate at 300μM for 30 min) to disrupt glial functions; n=6 (or more) animals; 2-way ANOVA and post hoc analysis using Sidak's multiple comparison test, *p<0.01; **p<0.001; ***p<0.0001).

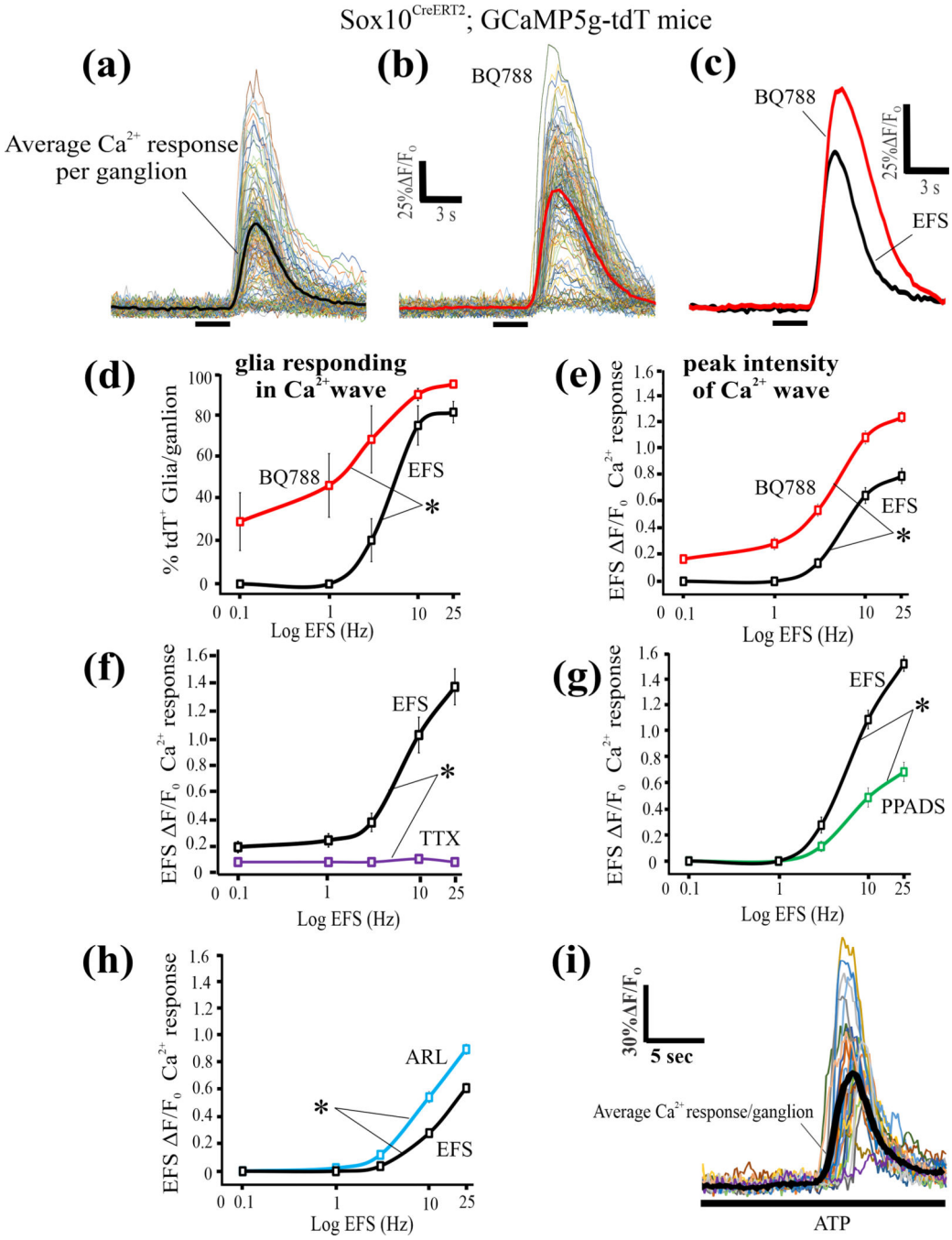

Figure 8. The physiological action of the selective ETB_R antagonist BQ788 is to enhance EFS-induced glial Ca^{2+} waves.

(a-i) EFS induced Ca^{2+} waves were studied in $Sox10^{CreERT2}$;GCaMP5g-tdT glial Ca^{2+}reporter mice. (a-c) A representative experiment in 1 animal showing that 1μM BQ788 superfusion of preparations for 30 min enhances the EFS (20Hz) Ca^{2+}wave response in glia of the intact myenteric plexus; individual cells are shown in (a) and (b) and the average response from all the glia/ganglionic field is shown in (c). (d, e) Blockade of ETB_R with BQ788 causes an increase in both the peak intensity of the Ca^{2+}response and the number of glia/ganglion responding in the EFS-induced Ca^{2+}wave. (f) The response to EFS is

abolished by 1μM TTX. (g) The response to EFS is partially blocked by the P2 receptor antagonist PPADS (30μM) confirming that purinergic signaling contributes to the EFS response [56]. (h) The ectonucleotidase inhibitor ARL67156 (200μM, 15 min superfusion) significantly augments EFS responses. (i) Exogenous ATP (100μM) that activates P2 receptors triggers a Ca^{2+}wave in enteric glia. *$p<0.01$.

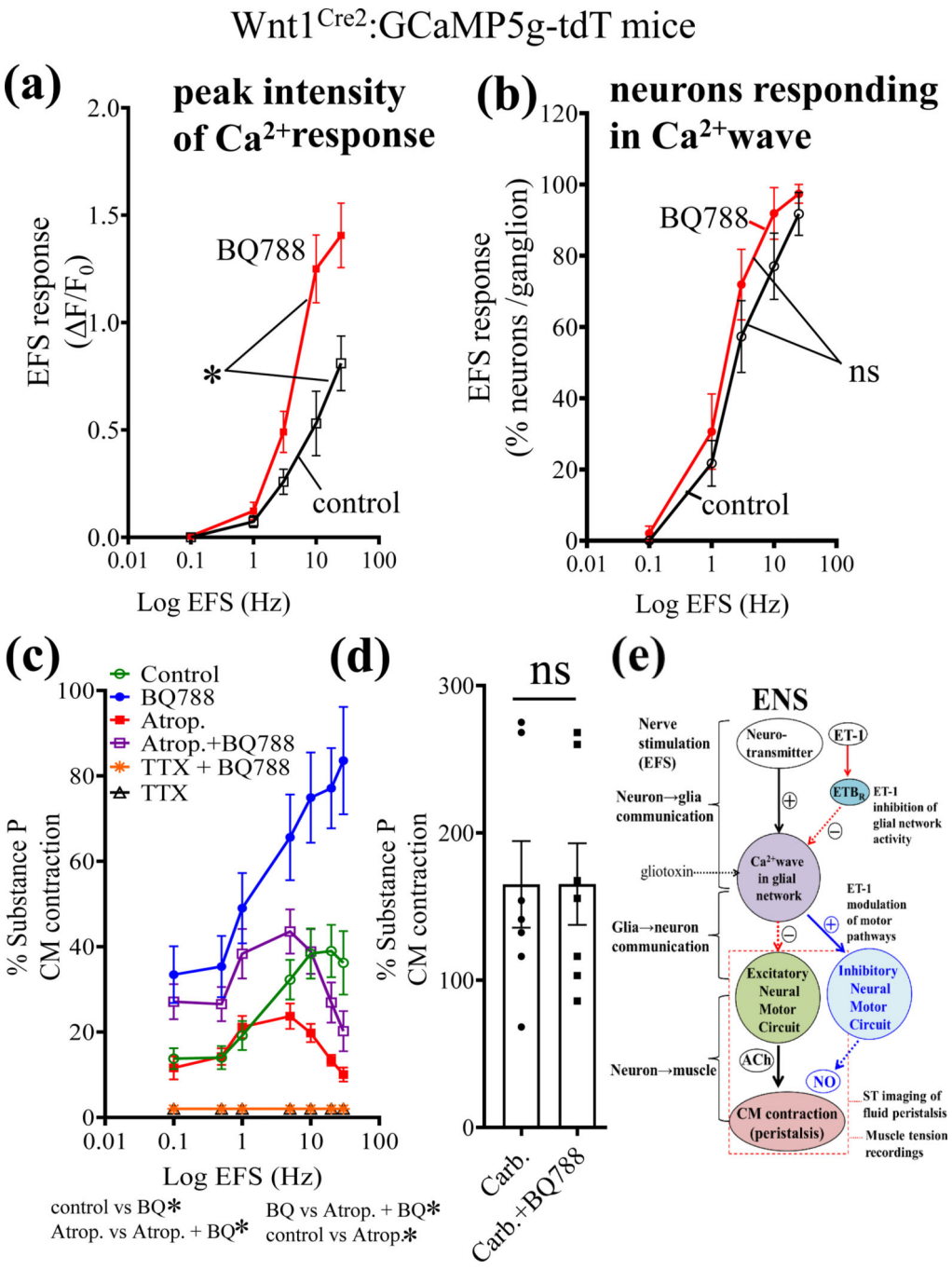

Figure 9. The physiological action of the ETB_R antagonist BQ788 is to enhance both ENS activation and excitatory cholinergic CM contractions.

(a-b) EFS induced Ca^{2+} waves in neurons were studied in $Wnt1^{Cre2}$;GCaMP5g-tdT Ca^{2+}reporter mice. (a) The peak intensity of the Ca^{2+}response was enhanced by BQ788 incubation for 30 min. (b) In contrast, the number of neurons/ganglion responding in the intact neural circuits was not influenced by BQ788. (c) The action of BQ788 is mitigated by the muscarinic antagonist atropine (10μM) used to block excitatory cholinergic CM contractions. (d) In contrast, BQ788 could not enhance or affect the direct muscle contraction caused by the muscarinic agonist carbachol (30μM, *p<0.01). For Fig. 9c,

*p<0.01; 2-way ANOVA using mixed effect model, n=8 or more animals for each group. For Fig. 9d; n=8 animals/group; ns, not significant). (e) Working model of the physiologic effect revealed by BQ788 on ET-1/ETB_R signaling in the ENS and motility. EFS nerve stimulation activates two distinct signaling pathways. First, it activates a stimulatory pathway in neurons to release transmitter(s) to trigger a glial Ca^{2+} wave. Purinergic signaling contributes to the neuron-to-glial communication as shown in previous reports[56]. Second, EFS activates the release of endogenous ET-1 from varicose nerve fibers to activate ETB_R in glia to inhibit glial Ca^{2+}waves. Glial Ca^{2+} waves modulate ENS activation of excitatory cholinergic motor pathways to muscle that regulate intestinal peristalsis. Evidence from the current study suggests that endogenous ET-1/ETB_R signaling inhibits excitatory neural motor circuits in the ENS involved in CM contractions and fluid induced peristaltic waves. Nitric oxide (NO) signaling could also be involved in the inhibitory mechanism. Overall, endogenous ET-1 may provide inhibitory modulation of excitatory glial motor pathways that can be revealed by pharmacological blockade of glial ETB_R with BQ788.

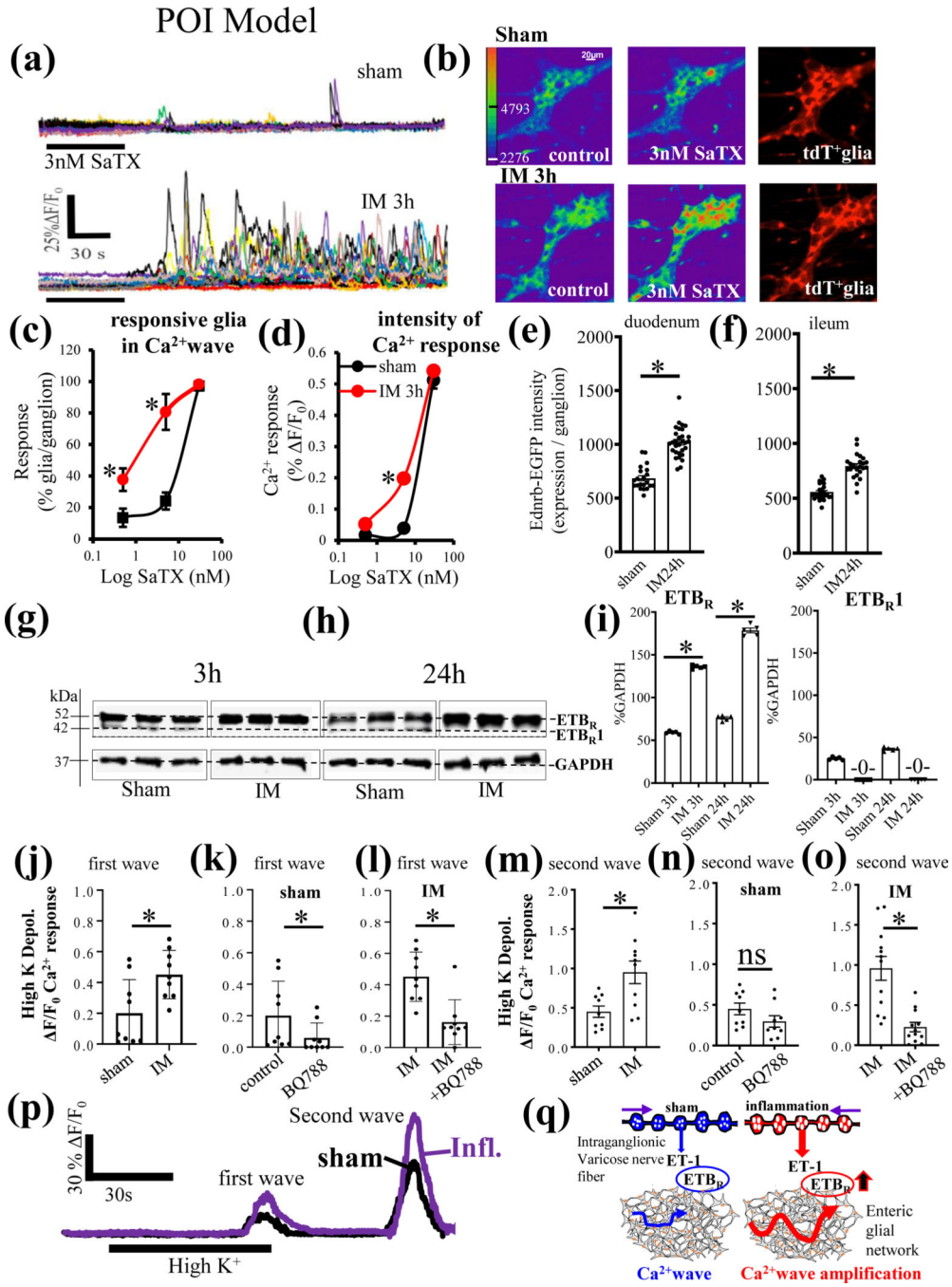

Figure 10. In a POI model of *muscularis externa* inflammation, ET-1 / ETB_R signaling is altered and upregulated after gut surgical trauma and manipulation.

(a-d) Hypersensitivity to the selective ETB_R agonist SaTX in enteric glia. (a) A concentration of 3nM SaTX causes a huge enhancement in the glial Ca^{2+} wave response. (b) Pseudocolor images show the enhanced Ca^{2+}response to SaTX in glia at 3h after intestinal manipulation (IM); tdT^+ glia in the $Sox10^{CreERT2}$;GCaMP5g-tdT Ca^{2+} reporter mice are used to identify responsive glia. (c-d) Pooled data showing SaTX hypersensitivity in both the number of glia/ganglion responding in the Ca^{2+}wave and the peak intensity of the Ca^{2+}response (*p<0.01); n=20 ganglia analyzed in separate perfusion experiments). (e-f)

Intestinal manipulation (IM 24h) caused increase in EGFP reporter fluorescence for the Ednrb-EGFP protein expression in the small intestine of the Tg(Ednrb-EGFP)EP59Gsat/Mmucd reporter mouse; (*p<0.01). (g-h) The expression of ETB_R in western blots of the *muscularis externa* is upregulated at 3h IM and 24h IM compared to sham-controls in wild-type mice. ETB_R1 is a lower molecular weight immunogenic band detected by the ETB_R antibody that is no longer present with IM. (i) Pooled data for the expression of ETB_R and ETB_R1 (arbitrary label) showing upregulation of ETB_R and absence of ETB_R1 after IM. (*p<0.01, n=5 animals/group). (j-o) Effects of BQ788 on high K^+ depolarization induced Ca^{2+}waves in $Sox10^{CreERT2}$;GCaMP5g-tdT Ca^{2+} reporter mice in sham and IM. (j) IM increases the peak Ca^{2+} response (ΔF/Fo) induced by high K^+ depolarization (*p<0.01) of the first wave (shown in 'p'). (k, l) BQ788 reduces the response in sham and IM – animals. (m) IM increases the peak Ca^{2+} response (ΔF/Fo) induced by high K^+ (*p<0.01) of the second wave. BQ788 reduces the second wave response to high K^+ in IM – animals (*p<0.01) but not sham animals. (p) Example of the Ca^{2+}response to high K^+depolarization in a single ganglion in sham versus IM (Inflamed) preparation; IM/Inflammation enhances the peak Ca^{2+}response (average glial Ca^{2+}response in a myenteric ganglion) of the first and second wave (n=10–12 ganglion experiments / group, *p<0.01). (q) Model of the effect of gut surgical manipulation (IM) on ET-1/ETB_R signaling in response to high K^+ depolarization. In sham-controls, high K^+ depolarization triggers 2 different Ca^{2+} waves separated by time. The Ca waves induced by high K^+ depolarization, are augmented by gut surgical manipulation (IM) and inflammation and responses are sensitive to blockade by the ETB_R antagonist BQ788, suggesting that there is a greater contribution of ET-1/ETB_R signaling to the Ca^{2+}wave produced by high K^+ depolarization in the inflamed state. Activity-dependent regulation of ETB_R signaling is revealed in POI.